

Drell-Yan forward-backward and spin asymmetries for arbitrary vector boson production at next-to-leading order

B. Kamal

Physics Department, Brookhaven National Laboratory, Upton, New York 11973, U.S.A.

(Submitted October 16, 1997 to Phys. Rev. D. In press.)

Longitudinally polarized, unpolarized and forward-backward mass differential cross sections for Drell-Yan lepton-pair production by arbitrary vector bosons are calculated in next-to-leading order (NLO) QCD. Analytical results are presented in a form valid for all consistent n -dimensional regularization schemes, with the mass factorization scheme kept general. NLO predictions for all Drell-Yan type processes (W^\pm , Z and γ^*) at BNL's relativistic heavy ion collider (RHIC) are made using polarized parton distributions which fit the recent deep-inelastic scattering data. These are examined as tools in the determination of the polarized parton distributions and the unpolarized \bar{u}/\bar{d} ratio. NLO predictions for the forward-backward lepton asymmetry at Fermilab are made and the precision determination of $\sin^2 \theta_W$ from future runs is studied. In all the above, the QCD corrections are found to be significant. An introductory discussion is given of various theoretical issues, such as allowable factorization and regularization schemes, and scale dependences.

12.38.Bx, 13.75.Cs, 13.85.Qk, 13.88.+e

I. INTRODUCTION

Two major areas of interest within the standard model are the determination of the polarized parton distributions of the proton and higher precision determinations of the electroweak mixing angle, $\sin^2 \theta_W$, as a constraint on the Higgs boson mass and new physics. One process useful in exploring both areas is Drell-Yan lepton-pair production. We shall present a clear picture of the Drell-Yan process at one-loop in QCD within a general framework which should be both instructive and useful. We will do so by considering the general interference between two vector bosons with arbitrary mass, width and couplings, which decay into a general lepton-antilepton pair (including neutrinos) and are produced via quark-antiquark fusion (one of the (anti)quarks may of course arise from an initial state gluon). In this way, we may consider possible new physics contributions, such as Z' bosons and four-fermion interactions, by appropriate choice of couplings, etc. . .

The emphasis here will be on presenting complete analytical results in a form valid for all consistent n -dimensional regularization schemes and within a general mass factorization framework. In addition, we will consider all possible longitudinal polarization states of the initial hadrons. Mass differential cross sections and asymmetries will be presented and the effect of the next-to-leading order (NLO) subprocesses will be highlighted and explained pedagogically. We will also discuss various constraints on allowed regularization and factorization schemes and describe the origin of the scale dependence of the one-loop corrected predictions in a general fashion.

The one-loop QCD corrections to the longitudinally polarized Drell-Yan process have been studied in several papers [1]–[5] using various regularization prescriptions (for the γ_5) and factorization schemes while considering the production by specific bosons. Here, we keep the formalism completely general. Results are kept in a simple form by considering explicitly only mass differential cross sections. As an application, we will study how lepton-pair production by γ^* , Z and W^\pm bosons can be used to extract the polarized parton distributions from forthcoming planned polarized pp collision experiments at BNL's relativistic heavy ion collider (RHIC), which is scheduled to start running in 1999. Longitudinally polarized pp collisions with both beams polarized are expected to begin in 2000 [6] with sufficient muon coverage to perform precision spin studies, in particular using W^\pm 's.

The QCD corrections are necessary in order to reduce the process dependence of the parton distributions. This allows comparison with and use of those distributions obtained in polarized deep-inelastic scattering (DIS). This form of global analysis will prove invaluable since, with the Drell-Yan process, we are sensitive to the sea-quark distributions, which are currently almost totally unconstrained from DIS. We can make use of the DIS determinations of the polarized valence distributions however, since we work consistently at NLO in QCD. Eventually RHIC will be able to improve those valence determinations due to the increased flavor separation in W^\pm production.

Another use of Drell-Yan at RHIC is a precision determination of the unpolarized \bar{u}/\bar{d} ratio at fairly large x and at very high energy scales where other experiments fall short. This can provide information on the limit $x \rightarrow 1$ at lower energy scales, via perturbative evolution. Similar statements apply to the polarized parton distributions with regard to the large- x sensitivity. All predictions will lie within the energy range $100 \text{ GeV} \leq \sqrt{s_{pp}} \leq 700 \text{ GeV}$, although RHIC, as currently envisioned, may not be able to run much above 500 GeV.

The Drell-Yan process also provides a useful way of obtaining $\sin^2 \theta_W$. One may ask why we would try to measure $\sin^2 \theta_W$ in hadron-hadron collisions when good measurements exist in Z production from e^+e^- annihilation at LEP and SLAC. The main reason is that these measurements are nearly complete. Future SLAC measurements will improve the earlier SLAC value, but a large discrepancy with the LEP measurement presently

exists and should not be expected to vanish. Thus, what is needed is an independent high precision measure of $\sin^2 \theta_W$. With various high luminosity scenarios planned for Fermilab's Run II [7], such a high precision measurement is indeed possible. This is because the forward-backward lepton asymmetry (in the lepton-pair rest frame) is sensitive to $\sin^2 \theta_W$. In a best case scenario, one could surpass the present (and future) average from LEP and SLAC combined. In a worst case scenario, a measurement at the same level of precision as the present SLAC measurement should be attainable. Various studies [8,7] have been done to show how such a high precision determination would significantly constrain the allowed mass region for the standard model Higgs and provide a probe of new physics.

QCD corrections to the charge asymmetry of lepton pairs produced in $p\bar{p}$ collisions have previously been investigated [9]. Unfortunately, the physical observables considered are not the ones used in determining $\sin^2 \theta_W$ and there does not appear to be any way to straightforwardly convert them into a useful form. Very recently, a paper appeared [10] performing detailed numerical studies of the QED and QCD corrections to the forward-backward Drell-Yan asymmetry in $p\bar{p}$ and pp collisions. There, Monte Carlo methods were used and similar results were obtained, even though a different definition of the forward-backward asymmetry beyond leading order was used, apparently in order to minimize the QCD corrections. As well, recently, soft gluon resummation effects on the lepton angular distribution from the decay of Z 's produced at the Fermilab Tevatron were briefly considered in [11]. Here, complete analytical results are presented for the mass differential cross sections and these do not appear elsewhere to our best knowledge. Also, hadron polarization effects as well as regularization and factorization scheme dependences are presented explicitly, which is not done elsewhere. One also sees quite clearly the structure of the QCD corrections and the origin of that structure.

The paper is organized as follows. In Section II we present our general formalism and describe the observables being considered. In Section III we discuss various features of dimensional regularization and dimensional reduction. In Sections IV–VI we compute the (singular) subprocess cross sections. In Section VII we perform the factorization of the mass singularities and discuss constraints on allowable regularization and factorization schemes. We also discuss how to convert subprocess cross sections and parton distributions from one scheme to another. In Section VIII we present the final analytical results and discuss the scale dependence issue in a general fashion. In Sections IX–XI we present numerical results relevant to RHIC and examine the sensitivity to the polarized parton distributions as well as the unpolarized \bar{u}/\bar{d} ratio. In Section XII we present the forward-backward Drell-Yan asymmetry relevant for the Fermilab Tevatron and discuss the extraction of $\sin^2 \theta_W$ from its measurement. Finally, in Section XIII we present our conclusions and summarize the work. Throughout, we have tried to avoid giving *standard* discussions of general issues in order to present new and more general perspectives which should be useful to non-experts.

II. GENERAL PROCESS AND FORMALISM

The Drell-Yan process with initial hadrons A, B of definite chirality is

$$A(P_1, \lambda_A) + B(P_2, \lambda_B) \rightarrow l(p_3) + \bar{l}(p_4) + X, \quad (1)$$

where λ_A, λ_B denote chiralities, \bar{l} represents a lepton pair and X is an arbitrary hadronic final state. We have the following invariant observables,

$$S \equiv (P_1 + P_2)^2, \quad M^2 \equiv q^2, \quad \tau \equiv M^2/S, \quad (2)$$

where

$$q = p_3 + p_4. \quad (3)$$

Denoting the y -axis as the direction of motion of hadron A , we may also define, in the c.m. of A and B , the observable

$$x_F \equiv \frac{2q_y}{\sqrt{S}}. \quad (4)$$

The general $2 \rightarrow 2$ [$2 \rightarrow 3$] parton subprocess contributing to (1) may be written as

$$\begin{aligned} & a(p_1, \lambda_1) + b(p_2, \lambda_2) \\ & \rightarrow B_i^*(q) + [c(k)] \rightarrow l(p_3) + \bar{l}(p_4) + [c(k)], \end{aligned} \quad (5)$$

where $B_i = \gamma, Z, W^\pm$ and $l = l^-, \nu_l$; $\bar{l} = l^+, \bar{\nu}_l$ (in the standard model). We must consider the cases $a = q, b = \bar{q}$, $c = g$; $a = \bar{q}, b = q, c = g$; $a = \overset{(-)}{q}, b = g, c = \overset{(-)}{q}$; $a = g, b = \overset{(-)}{q}, c = \overset{(-)}{q}$.

Using the parton model relations

$$p_1 = x_a P_1, \quad p_2 = x_b P_2, \quad (6)$$

we may define the subprocess invariants,

$$s \equiv (p_1 + p_2)^2 = x_a x_b S, \quad w \equiv \frac{M^2}{s} = \frac{M^2}{S x_a x_b} = \frac{\tau}{x_a x_b}, \quad (7)$$

where we took all external momenta to be massless, as usual. The parton momentum distributions are given by

$$F_k^{i/I}(x_i, \mu^2) = x_i f_k^{i/I}(x_i, \mu^2), \quad k = u, l, \quad (8)$$

where

$$f_u^{i/I}(x_i, \mu^2) = f_{+/+}^{i/I}(x_i, \mu^2) + f_{-/ +}^{i/I}(x_i, \mu^2) \quad (9)$$

and

$$f_l^{i/I}(x_i, \mu^2) = f_{+/+}^{i/I}(x_i, \mu^2) - f_{-/ +}^{i/I}(x_i, \mu^2). \quad (10)$$

Here $f_{\lambda_i/\lambda_I}^{i/I}(x_i, \mu^2)$ is the probability of finding parton i with chirality λ_i and momentum fraction x_i in hadron I having chirality λ_I , evaluated at renormalization scale μ^2 .

Introduce

$$z \equiv \cos \theta^*, \quad (11)$$

where θ^* is the angle between p_3 and P_1 (or, equivalently, p_1) in the $l\bar{l}$ rest frame. Then we may define

$$\sigma^{F\pm B} \equiv \int_0^1 dz \frac{d\sigma}{dz} \pm \int_{-1}^0 dz \frac{d\sigma}{dz}. \quad (12)$$

Hence σ^{F+B} has the interpretation as the usual leptonic integrated cross section. We call σ^{F-B} the *forward-backward* cross section.

Let $\sigma^{ab}(\lambda_a, \lambda_b)$ denote the cross section for colliding partons (or hadrons with some degree of polarization) a, b having chiralities (or beam polarization directions) λ_a, λ_b . Then there are only 4 combinations of λ_a, λ_b leading to well factorized parton model expressions, as may be straightforwardly verified. All other observables may be expressed in terms of these. They are

$$\sigma_{uu}^{ab} \equiv \frac{1}{4} [\sigma^{ab}(+, +) + \sigma^{ab}(+, -) + \sigma^{ab}(-, +) + \sigma^{ab}(-, -)] \quad (13)$$

$$\sigma_{lu}^{ab} \equiv \frac{1}{4} [\sigma^{ab}(+, +) + \sigma^{ab}(+, -) - \sigma^{ab}(-, +) - \sigma^{ab}(-, -)] \quad (14)$$

$$\sigma_{ul}^{ab} \equiv \frac{1}{4} [\sigma^{ab}(+, +) - \sigma^{ab}(+, -) + \sigma^{ab}(-, +) - \sigma^{ab}(-, -)] \quad (15)$$

$$\sigma_{ll}^{ab} \equiv \frac{1}{4} [\sigma^{ab}(+, +) - \sigma^{ab}(+, -) - \sigma^{ab}(-, +) + \sigma^{ab}(-, -)]. \quad (16)$$

The notation is straightforward: σ_{mn}^{ab} denotes the cross section when a has polarization m and b has polarization n . In shorthand,

$$u = (\lambda = +) + (\lambda = -), \quad l = (\lambda = +) - (\lambda = -), \quad (17)$$

so that u denotes unpolarized and l denotes longitudinally polarized. The factor $1/4$ is required so that σ_{uu} has the interpretation as the spin averaged cross section.

The parton model expression for the mass differential Drell-Yan cross section, for general beam polarization, is

$$\begin{aligned} \frac{d\sigma_{mn}^{AB, F\pm B}}{dM} &= \mathcal{S}_m^A \mathcal{S}_n^B \sum_{ab} \int_{\tau}^1 dx_a \int_{\tau/x_a}^1 dx_b f_m^{a/A}(x_a, \mu^2) f_n^{b/B}(x_b, \mu^2) \frac{d\hat{\sigma}_{mn}^{ab, F\pm B}}{dM} \\ &= \mathcal{S}_m^A \mathcal{S}_n^B \sum_{ab} \int_{\tau}^1 \frac{dx_a}{x_a} \int_{\tau/x_a}^1 \frac{dw}{w} F_m^{a/A}(x_a, \mu^2) F_n^{b/B}(x_b, \mu^2) \frac{d\hat{\sigma}_{mn}^{ab, F\pm B}}{dM} \\ &= \mathcal{S}_m^A \mathcal{S}_n^B \sum_{ab} \int_{-(1-\tau)}^{1-\tau} dx_{F0} \int_{w_1}^1 \frac{dw}{w} \frac{1}{x_a + x_b} F_m^{a/A}(x_a, \mu^2) F_n^{b/B}(x_b, \mu^2) \frac{d\hat{\sigma}_{mn}^{ab, F\pm B}}{dM}, \end{aligned} \quad (18)$$

where

$$x_{F0} \equiv x_a - x_b, \quad w_1 = \frac{\tau}{1 - |x_{F0}|}, \quad x_{a,b} = \frac{\sqrt{x_{F0}^2 + 4\tau/w} \pm x_{F0}}{2}. \quad (19)$$

$\hat{\sigma}^{ab}$ is the subprocess cross section corresponding to (5) and

$$\mathcal{S}_u^I = 1, \quad \mathcal{S}_l^I = \mathcal{P}^I, \quad (20)$$

where \mathcal{P}^I is the degree of polarization of the beam of hadrons I . The only assumption made in the derivation of (18) is that the degree of beam polarization is the same in both polarization directions. The same factors of beam polarization will always enter, regardless of the specific differential cross section being considered. The experimental results (for the σ_{mn}) will have to be divided by the appropriate factors of beam polarization in constructing asymmetries. In general, this is unavoidable since the beam polarization will vary as a function of time for any given experiment. In numerical calculations taking evenly spaced integration points (i.e. Simpson's rule) the third form of (18) is most convenient because x_a and x_b are integrated over symmetrically while the inner integral is over w and $d\hat{\sigma}/dM$ contains functions singular in $1-w$ (i.e. $\delta(1-w)$, $1/(1-w)_+$, \dots).

We will consider lepton-pair production by N arbitrary vector bosons, B_i , having masses M_i , widths Γ_i and couplings to fermions given by

$$ic_f^i \gamma^\alpha (g_{vf}^i - g_{af}^i \gamma_5). \quad (21)$$

Hence we may write

$$\frac{d\hat{\sigma}_{mn}^{ab, F \pm B}}{dM} = \sum_{i \geq j} \frac{d\hat{\sigma}_{mn, B_i B_j}^{ab, F \pm B}}{dM}, \quad (22)$$

where $\hat{\sigma}_{mn, B_i B_j}^{ab, F \pm B}$ is the total interference contribution from B_i , B_j (i.e. for $i \neq j$ it is the sum over the i, j and j, i contributions). For $M, \Gamma, g_A \rightarrow 0$ we obtain the photon contribution so that the argumentation is completely general. This formalism applies to Z and W^\pm production and the Drell-Yan production of any bosons whose coupling to fermions is given by (21), provided there are no new contributing diagrams. This includes non standard model Z' and $W^{\pm'}$ contributions. As well, we can include four-fermion interactions. For W^\pm production, the c_f^i will depend on both quark flavors at the vertex via the appropriate CKM matrix element.

The normalization convention of our squared amplitudes is easily inferred from the standard leading order parton model cross section expression,

$$\begin{aligned} \frac{d\sigma_{mn}^{AB}}{dM dx_F dz} &= \frac{1}{\pi M^3} \frac{\mathcal{S}_m^A \mathcal{S}_n^B}{x_a + x_b} \sum_{ab} F_m^{a/A}(x_a, \mu^2) F_n^{b/B}(x_b, \mu^2) \\ &\times \sum_{i \geq j} |M|_{mn, B_i B_j}^{2ab}, \end{aligned} \quad (23)$$

where

$$ab = q\bar{q}, \bar{q}q, \quad x_F = x_{F0} \quad (24)$$

and $|M|_{mn, B_i B_j}^{2ab}$ denotes the net interference between the amplitude involving B_i and that involving B_j . This corresponds to the convention $\sum_\lambda u(p, \lambda) \bar{u}(p, \lambda) = \not{p}/2$ for $p^2 = 0$, which we maintain for consistency with [4].

As far as QCD corrections are concerned, we will only consider $d\sigma/dM$. In imposing experimental cuts, one restricts the phase space of the outgoing leptons. Since the QCD corrections effect the hadronic sector, the features of the corrections should not be greatly influenced by the leptonic cuts. In the limit of small cuts (i.e. good leptonic coverage) the expressions in this paper become exact. We will not address further the issue of leptonic cuts in what follows.

III. n -DIMENSIONAL REGULARIZATION SCHEME PECULIARITIES

Since we will need to present the leading order (LO) cross sections in n ($\equiv 4 - 2\epsilon$) dimensions in the next section, it is appropriate to discuss the various n -dimensional regularization schemes at this point. We will consider regularization by dimensional regularization (DREG) [12,13] and by dimensional reduction (DRED) [14].

In [4], the details concerning DREG and DRED were summarized and will not be repeated here. The important points will be discussed however. Within DREG, there are two commonly used schemes for dealing with the γ_5 matrix (and $\varepsilon^{\mu\nu\rho\sigma}$ tensor) which arises in polarized processes. In the 't Hooft-Veltman-Breitenlohner-Maison (HVBM) scheme [12,15], all quantities are mathematically well-defined, but the non-anticommuting γ_5 leads to physical problems. These necessitate finite renormalizations of the polarized parton distributions and UV counterterms (for non QCD/QED vertices) as will be discussed throughout this paper. In the anticommuting- γ_5 scheme [16], massless quark helicity is conserved, but only at the expense of mathematical consistency when an odd number of γ_5 's arise in the traces. Also, one needs to devise prescriptions [17] for dealing with the $\varepsilon^{\mu\nu\rho\sigma}$

tensor (arising from polarized gluons), since nothing other than the HVBM definition has been proven to be mathematically consistent in DREG.

Even when performing calculations where only an even number of γ_5 's occur in the traces, one may wonder if the result is meaningful in general, using an anticommuting γ_5 . For the case of longitudinal polarization, the γ_5 is connected with helicity, and we understand the need for helicity conservation on physical grounds. For processes such as the transverse Drell-Yan process, the γ_5 also arises. Here though, there is no physical motivation for using an anticommuting γ_5 in DREG, other than that it simplifies calculations. More study is required in this area since recently two-loop transversity splitting functions have been calculated by three groups [18–20] using an anticommuting γ_5 . The transverse case is somewhat more subtle than the longitudinal case, however, due to the additional axis which enters. We do not consider transversity further in this work.

So, in general, the anticommuting- γ_5 scheme [16] should only be used in situations where it is physically motivated. And in those situations, it should always be shown that the same results can be obtained using the HVBM scheme via finite renormalizations of the parton distributions or by the addition of UV counterterms. The above renormalizations and UV counterterms should be unique (in any given gauge) for some class of subprocesses. This is the approach we will follow in this paper. All results are understood to refer to consistent schemes: those schemes which can be related to the HVBM scheme as described above. Hence, we will always refer to the HVBM result as being the DREG result.

More recently, a γ_5 scheme was introduced [21] which reproduces many of the desirable features of the HVBM scheme, such as the correct ABJ anomaly, and claims mathematical consistency without violating helicity conservation. This scheme uses a *reading point* (a specific leftmost γ -matrix in the trace) and maintains an anticommuting γ_5 , which requires non-cyclicity of the traces. What remains, therefore, is to show that this scheme leads to process independent n -dimensional splitting functions. This will be discussed below.

Because of the tedious nature of the HVBM scheme, and the other problems mentioned earlier, it is more straightforward to first use DRED to calculate subprocess cross sections, then present them in a form valid for all consistent n -dimensional regularization schemes using the technique of [4]. The only drawback is that one has to add a UV counterterm to the quark- $\gamma(Z, W^\pm)$ vertex when using DRED. Fortunately, this counterterm is well established and unambiguous.

The DRED result for a physical cross section is (formally speaking) defined as the result obtained by contracting all tensors and taking all traces in 4 dimensions, then performing all phase space integrals in n dimensions (and adding any necessary UV counterterms). When considering QCD/QED corrections, one needn't actually take the traces first. One may work directly at the amplitude level for loop diagrams. For other theories, however, like supersymmetry, the ill-definedness of $g_n^{\mu\nu}$ for noninteger $n < 4$ leads to an ambiguity such that the results may depend on the order of operations [22]. In the HVBM scheme ($n > 4$), $g_n^{\mu\nu}$ is defined since there are an infinite number of integer dimensions with $n > 4$. Hence we may continue $g_n^{\mu\nu}$ to $n > 4$ by simply using relations valid in integer dimensions, but take the continuous limit $n \rightarrow 4$ on the real axis (or complex plane) at the end of the calculation (i.e. after all divergences have been cancelled), as if one compressed the infinite number of dimensions into a continuum for $n > 4$. In practice, of course, one continues to noninteger n from the beginning rather than at the end. As there are a finite number of dimensions with $n < 4$, we cannot continue $g_n^{\mu\nu}$ into the region $n < 4$. Hence, strictly speaking, we must first perform all contractions and traces in 4 dimensions, then go to n dimensions to perform the phase space integrals, since only scalar products of vectors will remain, which are manifestly continuable to n dimensions. In that way, $g_n^{\mu\nu}$ will never be contracted into traces containing γ_5 or with $\varepsilon^{\mu\nu\rho\sigma}$, which is where the ambiguity could arise.

In order to present $d\hat{\sigma}_{mn}^{ab,F\pm B}/dM$ in a form valid for all consistent n -dimensional schemes, we must first give the general form of the n -dimensional Altarelli-Parisi [23] splitting functions, $P_{ij}^n(z)$, related to the probability of parton j splitting into a collinear parton i having momentum fraction z , plus an arbitrary final state carrying the rest of the momentum. The reason is that the regularization scheme dependences arising from mass singularities are entirely contained in these functions, as was shown in [4] (and references therein). Hence, we discuss them here. We may write

$$P_{ij}^n(z, \varepsilon) \equiv P_{ij}^4(z) + \varepsilon P_{ij}^\varepsilon(z), \quad (25)$$

where $P_{ij}^4(z)$ is the usual 4-dimensional splitting function. In DRED,

$$P_{ij}^{n,\text{DRED}}(z, \varepsilon) = P_{ij}^4(z). \quad (26)$$

We will also use the notation,

$$P_{ij}^n(z, \varepsilon) \equiv P_{ij}^{n,<}(z, \varepsilon) + \delta(1-z)P_{ij}^{n,\delta}(\varepsilon), \quad (27)$$

and define

$$\Delta_u P_{ij} \equiv P_{ij,++} + P_{ij,-+}, \quad \Delta_t P_{ij} \equiv P_{ij,++} - P_{ij,-+}, \quad (28)$$

where the $+$, $-$ denote the respective chiralities.

In DREG, the unpolarized one-loop splitting functions are given by [24]

$$\begin{aligned}
\Delta_u P_{qq}^4(z) &= C_F \left[\frac{2}{(1-z)_+} - 1 - z + \frac{3}{2}\delta(1-z) \right], & \Delta_u P_{qq}^\varepsilon(z) &= C_F \left[-(1-z) + \frac{1}{2}\delta(1-z) \right], \\
\Delta_u P_{qg}^4(z) &= \frac{1}{2}(1-2z+2z^2), & \Delta_u P_{qg}^\varepsilon(z) &= z^2 - z, \\
\Delta_u P_{gq}^4(z) &= C_F \left[\frac{2}{z} - 2 + z \right], & \Delta_u P_{gq}^\varepsilon(z) &= -C_F z, \\
\Delta_u P_{gg}^4(z) &= 2N_C \left[\frac{1}{(1-z)_+} + \frac{1}{z} - 2 + z(1-z) \right] + \frac{\beta_0}{2}\delta(1-z), & \Delta_u P_{gg}^\varepsilon(z) &= \frac{N_F}{6}\delta(1-z),
\end{aligned} \tag{29}$$

where $\beta_0 = \frac{11}{3}N_C - \frac{2}{3}N_F$ and the usual convention of $2-2\varepsilon$ ($=n-2$) gluon polarization states was used. In fact, the latter is somewhat more than a convention, since it is justified on physical grounds.

Within DREG, we need only consider longitudinally polarized splitting functions determined in the HVBM scheme since, at present, it is the only established mathematically consistent scheme therein, which also leads to process independent n -dimensional splitting functions. At one-loop they are given by

$$\begin{aligned}
\Delta_l P_{qq}^4(z) &= \Delta_u P_{qq}^4(z), & \Delta_l P_{qq}^\varepsilon(z) &= C_F \left[3(1-z) + \frac{1}{2}\delta(1-z) \right], \\
\Delta_l P_{qg}^4(z) &= z - 1/2, & \Delta_l P_{qg}^\varepsilon(z) &= -(1-z), \\
\Delta_l P_{gq}^4(z) &= C_F(2-z), & \Delta_l P_{gq}^\varepsilon(z) &= 2C_F(1-z), \\
\Delta_l P_{gg}^4(z) &= 2N_C \left[\frac{1}{(1-z)_+} - 2z + 1 \right] + \frac{\beta_0}{2}\delta(1-z), & \Delta_l P_{gg}^\varepsilon(z) &= 4N_C(1-z) + \frac{N_F}{6}\delta(1-z),
\end{aligned} \tag{30}$$

as can be inferred from [25].

These n -dimensional splitting functions were determined by investigating the factorization properties of the NLO squared amplitudes in various collinear limits for various subprocesses. In [25] it was found that one always obtains a Born term multiplied by the appropriate n -dimensional splitting function in the limit where two partons are collinear, leading to a pole in a propagator. It is important that the Born term be exactly the n -dimensional one appropriate to the regularization scheme in question; in the above case, HVBM. We investigated what happens in the scheme of [21] for the qg subprocess of longitudinally polarized Drell-Yan. For simplicity, we chose the γ_5 coming from the polarized incoming quark as reading point. We found that the wrong Born term arose, in the collinear limit where the outgoing quark is collinear with the initial state gluon. Namely, that of HVBM rather than that of [21]. The basic reason is that the squared amplitude for the qg subprocess in the scheme of [21] is equivalent to the HVBM result, with our choice of reading point. Hence, in the collinear limit, the Born term ($q\bar{q}$) and n -dimensional splitting function ($\Delta_l P_{qg}^n$) which arise correspond to the HVBM ones. Unfortunately, the Born term for the $q\bar{q}$ subprocess in the scheme of [21] demands an anticommuting γ_5 , hence the result is simply minus the unpolarized one. This is not true in HVBM, due to the non-anticommuting γ_5 . Hence the Born terms are different in the two schemes and the behaviour of the qg squared amplitude in the collinear limit is unphysical. This physical inconsistency is clearly unacceptable and it will lead to process dependent n -dimensional splitting functions. A different choice of reading point might rectify the situation, but such an ambiguity is also unacceptable. Unfortunately, the prescription of [21] gives no unambiguous definition of what the reading point should be in all cases. Therefore some extension is in order before it can be applied in practical QCD corrections to polarized processes. We will not discuss the scheme of [21] in further detail.

The only subtlety associated with calculating the $\Delta_l P_{ij}^n$ in the HVBM scheme is that one must additionally perform an integration over the \hat{k} momenta (i.e. the components between 4 and n dimensions), rather than simply taking a collinear limit [4] as is done in anticommuting- γ_5 schemes and in the unpolarized case. One still obtains process independent splitting functions since the collinear phase space structure is process independent. Even in some anticommuting- γ_5 schemes [17], one must resort to Sudakov kinematics in the collinear limit, making the process nontrivial. In that case, one must drop certain potentially finite terms of $\mathcal{O}(\varepsilon)$ which only vanish after integration.

In what follows, we shall present tensors and squared amplitudes calculated using DRED. Then, using the method of [4], we present the necessary one-loop subprocess cross sections in a form valid for all consistent n -dimensional regularization schemes. By “ n -dimensional regularization schemes”, we mean schemes in which all divergences are regularized by dimensional continuation. This excludes all forms of off-shell and cutoff regularization schemes which also involve dimensional continuation to regularize some of the divergences. The mass factorization scheme will be kept general.

IV. LEADING ORDER CROSS SECTIONS

Unless otherwise stated, the expressions presented here are calculated using DRED. The unintegrated leptonic tensor $L_{BB'}^{\alpha\beta}$ is defined as the product of L_B^α and $L_{B'}^{\beta*}$, where L_B^α is the leading order amplitude consisting of a lepton pair attached to boson B at a vertex having index α . It is given by

$$L_{BB'}^{\alpha\beta} = \frac{\mu^{2\varepsilon}}{4} c_l c_l' [(g_{vl} g_{vl}' + g_{al} g_{al}') T_{1l}^{\alpha\beta} - (g_{al} g_{vl}' + g_{vl} g_{al}') T_{2l}^{\alpha\beta}], \quad (31)$$

with

$$\begin{aligned} T_{1l}^{\alpha\beta} &= 4(p_3^\alpha p_4^\beta + p_4^\alpha p_3^\beta - \frac{M^2}{2} g^{\alpha\beta}), \\ T_{2l}^{\alpha\beta} &= 4i\varepsilon^{\alpha\beta\mu\nu} p_{3\mu} p_{4\nu}, \end{aligned} \quad (32)$$

where the arbitrary mass scale $\mu^{2\varepsilon}$ arises from the n -dimensional coupling $e^2 \rightarrow e^2 \mu^{2\varepsilon}$. Since μ is arbitrary, the physical predictions should not depend on it, order by order in α_s . We will show how this is explicitly satisfied at one-loop in section VIII.

Now define the integrated leptonic tensor as

$$\mathcal{L}_{F+B}^{\alpha\beta} = \overbrace{\int \frac{d^{n-1} p_3}{(2\pi)^{n-1} 2p_{3,0}} \frac{\delta[(q-p_3)^2]}{q^2}}^{\equiv \int_{F+B} \mathcal{D}p_3} L^{\alpha\beta}. \quad (33)$$

Here we omitted the BB' indices, and will often do so for compactness. One finds [4]

$$\mathcal{L}_{F+B}^{\alpha\beta} = \kappa \left[(1-\varepsilon) \frac{q^\alpha q^\beta}{q^2} + \frac{g_n^{\alpha\beta}}{2} - (3-2\varepsilon) \frac{g^{\alpha\beta}}{2} \right], \quad (34)$$

where κ now generalizes to

$$\kappa = c_l c_l' \frac{\mu^{2\varepsilon}}{2^{4-2\varepsilon}} \frac{(q^2)^{-\varepsilon}}{\pi^{2-\varepsilon}} \frac{\Gamma(1-\varepsilon)}{\Gamma(1-2\varepsilon)} \frac{(g_{vl} g_{vl}' + g_{al} g_{al}')}{(3-2\varepsilon)(1-2\varepsilon)}. \quad (35)$$

It is interesting to note that the corresponding DREG tensor, in an anticommuting- γ_5 scheme, is obtained by replacing $g^{\alpha\beta} \rightarrow g_n^{\alpha\beta}$. This gives

$$\mathcal{L}_{F+B, \text{DREG}}^{\alpha\beta} = \kappa(1-\varepsilon) \left[\frac{q^\alpha q^\beta}{q^2} - g_n^{\alpha\beta} \right]. \quad (36)$$

Of course, $T_{2l}^{\alpha\beta}$ is not defined in such a scheme, but it does not contribute here. In all schemes, the part $\sim q^\alpha q^\beta$ does not contribute to the cross section, as follows from gauge invariance. $\mathcal{L}_{F+B}^{\alpha\beta}$ is thus effectively a constant tensor. We nonetheless keep all the terms for completeness.

We may define the forward-backward integrated leptonic tensor with respect to an arbitrary massless vector, p , in a covariant fashion using

$$\mathcal{L}_{F-B(p)}^{\alpha\beta} \equiv \int_{F+B} \mathcal{D}p_3 [\theta(p \cdot q/2 - p \cdot p_3) - \theta(p \cdot p_3 - p \cdot q/2)] L^{\alpha\beta} \quad (37)$$

$$\equiv \int_{F-B(p)} \mathcal{D}p_3 L^{\alpha\beta} \quad (38)$$

$$= -\bar{\kappa} i \varepsilon^{\alpha\beta\mu\nu} \frac{p_\mu q_\nu}{2p \cdot q}, \quad (39)$$

where θ is the step function and

$$\bar{\kappa} = c_l c_l' \frac{\mu^{2\varepsilon}}{2^{5-2\varepsilon}} \frac{(q^2)^{-\varepsilon}}{\pi^{2-\varepsilon}} \frac{\Gamma(1-\varepsilon)}{\Gamma(1-2\varepsilon)} F(\varepsilon) (g_{al} g_{vl}' + g_{vl} g_{al}'), \quad (40)$$

with

$$\begin{aligned} F(\varepsilon) &\equiv 4 \frac{\Gamma(1-2\varepsilon)}{\Gamma^2(1-\varepsilon)} \int_0^{1/2} dy [y^{-\varepsilon} (1-y)^{1-\varepsilon} \\ &\quad - y^{1-\varepsilon} (1-y)^{-\varepsilon}] = 1 + \mathcal{O}(\varepsilon). \end{aligned} \quad (41)$$

The most general tensor structure of $\mathcal{L}_{F-B(p)}^{\alpha\beta}$ may be obtained by noting that only the antisymmetric part of $L^{\alpha\beta}$ contributes. Hence $\mathcal{L}_{F-B(p)}^{\alpha\beta}$ must be antisymmetric in α, β and can only depend on the momenta p and q . Then one uses the usual projection methods, as was done to obtain (34). We will use the notation

$$\mathcal{L}_{F-B}^{\alpha\beta} \equiv \mathcal{L}_{F-B(p_1)}^{\alpha\beta}, \quad \int_{F-B} \mathcal{D}p_3 \equiv \int_{F-B(p_1)} \mathcal{D}p_3. \quad (42)$$

It is easy to check that (37) leads to the usual definition of the forward-backward asymmetry, Eq. (12), by working in the rest frame of q . Choices of reference axes other than p_1 are of course possible, but using p_1 allows a straightforward, covariant treatment. Having performed the forward-backward leptonic integration analytically greatly simplifies the next-to-leading order calculation.

We may next define the subprocess hadronic tensor $W_{ab,BB'}^{\alpha\beta}$ through the subprocess squared Feynman amplitude contribution from B, B' interference,

$$|M|_{ab,BB'}^2 \equiv D_{BB'}^{-1} L_{\alpha\beta}^{BB'} W_{ab,BB'}^{\alpha\beta} (2 - \delta_{BB'}), \quad (43)$$

where

$$D_{BB'}^{-1} \equiv \frac{(M^2 - M_B^2)(M^2 - M_{B'}^2) + M_B M_{B'} \Gamma_B \Gamma_{B'}}{[(M^2 - M_B^2)(M^2 - M_{B'}^2) + M_B M_{B'} \Gamma_B \Gamma_{B'}]^2 + [M_B \Gamma_B (M^2 - M_{B'}^2) - M_{B'} \Gamma_{B'} (M^2 - M_B^2)]^2}. \quad (44)$$

For $a = q, b = \bar{q}$, the leading order hadronic tensor is

$$W_{q\bar{q}}^{\alpha\beta} = \frac{\mu^{2\varepsilon}}{2^4 N_C} c_q c'_q \{ (g_{vq} g'_{vq} + g_{aq} g'_{aq}) [T_{1h}^{\alpha\beta} (1 - \lambda_1 \lambda_2) + T_{2h}^{\alpha\beta} (\lambda_1 - \lambda_2)] \\ - (g_{aq} g'_{vq} + g_{vq} g'_{aq}) [T_{1h}^{\alpha\beta} (\lambda_1 - \lambda_2) + T_{2h}^{\alpha\beta} (1 - \lambda_1 \lambda_2)] \}, \quad (45)$$

where

$$T_{1h}^{\alpha\beta} = 4(p_1^\alpha p_2^\beta + p_2^\alpha p_1^\beta - \frac{M^2}{2} g^{\alpha\beta}), \quad T_{2h}^{\alpha\beta} = -4i\varepsilon^{\alpha\beta\mu\nu} p_{1\mu} p_{2\nu}. \quad (46)$$

Using (31) and (45) in (43) gives the LO result for $a = q, b = \bar{q}$,

$$|M|_{q\bar{q},BB'}^2(z) \\ = (2 - \delta_{BB'}) D_{BB'}^{-1} \frac{\mu^{4\varepsilon} M^4}{2^4 N_C} c_l c'_l c_q c'_q \{ (1 - \lambda_1 \lambda_2) [(g_{vl} g'_{vl} + g_{al} g'_{al})(g_{vq} g'_{vq} + g_{aq} g'_{aq})(1 + z^2) \\ + 2(g_{al} g'_{vl} + g_{vl} g'_{al})(g_{aq} g'_{vq} + g_{vq} g'_{aq})z] + (\lambda_2 - \lambda_1) [(g_{vl} g'_{vl} + g_{al} g'_{al}) \\ \times (g_{aq} g'_{vq} + g_{vq} g'_{aq})(1 + z^2) + 2(g_{al} g'_{vl} + g_{vl} g'_{al})(g_{vq} g'_{vq} + g_{aq} g'_{aq})z] \}. \quad (47)$$

This reproduces the result of [26] which includes the effect of Z' bosons in the Drell-Yan process. We may express the above in a covariant fashion using

$$z = (u^2 - t^2)/M^2, \quad 1 + z^2 = 2(t^2 + u^2)/M^2, \\ t \equiv (p_1 - p_3)^2 = (p_2 - p_4)^2, \quad u \equiv (p_2 - p_3)^2 = (p_1 - p_4)^2. \quad (48)$$

Defining

$$\mathcal{M}_{ab,BB'}^{F\pm B} \equiv \int_{F\pm B} \mathcal{D}p_3 L_{\alpha\beta}^{BB'} W_{ab,BB'}^{\alpha\beta} = \mathcal{L}_{\alpha\beta}^{BB',F\pm B} W_{ab,BB'}^{\alpha\beta}, \quad (49)$$

we have, for $a = q, b = \bar{q}$ and in leading order,

$$\mathcal{M}_{q\bar{q}}^{F+B} = \frac{\mu^{2\varepsilon} M^2}{2^3 N_C} c_q c'_q \kappa (2 - \varepsilon) [(g_{vq} g'_{vq} + g_{aq} g'_{aq})(1 - \lambda_1 \lambda_2) + (g_{aq} g'_{vq} + g_{vq} g'_{aq})(\lambda_2 - \lambda_1)] \quad (50)$$

and

$$\mathcal{M}_{q\bar{q}}^{F-B} = \frac{\mu^{2\varepsilon} M^2}{2^3 N_C} c_q c'_q \bar{\kappa} [(g_{aq} g'_{vq} + g_{vq} g'_{aq})(1 - \lambda_1 \lambda_2) + (g_{vq} g'_{vq} + g_{aq} g'_{aq})(\lambda_2 - \lambda_1)], \quad (51)$$

where we used (34) and (39), respectively, in (49). The correctness of this approach (i.e. integrating over the leptonic tensor first, then contracting the leptonic and hadronic tensors) was verified by contracting first, then performing the leptonic integration. One obtains exactly the same result, in n dimensions.

This is straightforwardly checked by noting that, in the rest frame of q ,

$$\int_{F+B} \mathcal{D}p_3 \rightarrow \frac{1}{2^{5-2\varepsilon}} \frac{(q^2)^{-1-\varepsilon}}{\pi^{3-\varepsilon}} \frac{\Gamma(1-\varepsilon)}{\Gamma(1-2\varepsilon)} \int d^2\omega_3, \quad (52)$$

where

$$\int d^2\omega_3 = \int_0^\pi d\theta_1 \sin^{1-2\varepsilon} \theta_1 \int_0^\pi d\theta_2 \sin^{-2\varepsilon} \theta_2 \quad (53)$$

and the θ_i represent the first two of the $n - 2$ angles of p_3 in n dimensions [27] and θ_1 is taken to be the angle between p_3 and p_1 (i.e. θ^*). Since $|M|^2$ does not depend on θ_2 ,

$$\int d^2\omega_3 \rightarrow 2\pi \frac{\Gamma(1-2\varepsilon)}{\Gamma^2(1-\varepsilon)} \int_0^1 dy y^{-\varepsilon} (1-y)^{-\varepsilon}, \quad y \equiv \frac{1+z}{2}. \quad (54)$$

We simply make the substitutions,

$$z = y - (1-y), \quad 1+z^2 = 2 - 4y(1-y), \quad (55)$$

in (47), then integrate over y .

The $2 \rightarrow 2$ phase space is

$$\left(\frac{d\hat{\sigma}_{mn,BB'}^{ab,F\pm B}}{dM} \right)_{\text{LO}} = \frac{32\pi}{M} \delta(1-w) \int_{F\pm B} \mathcal{D}p_3 |M|_{mn,BB'}^{2ab} \quad (56)$$

$$= \frac{32\pi}{M} D_{BB'}^{-1} \mathcal{M}_{mn,BB'}^{ab,F\pm B} (2 - \delta_{BB'}) \delta(1-w) \equiv \chi_{mn,BB'}^{ab,F\pm B}(\varepsilon) \delta(1-w). \quad (57)$$

χ has the form

$$\chi_{mn,BB'}^{ab,F\pm B}(\varepsilon) = (2 - \delta_{BB'}) \frac{M}{2\pi N_C} \frac{c_q c'_q c_l c'_l}{D_{BB'}} K_{BB'}^{l^+ l^-, F\pm B} F_{mn,BB'}^{ab,F\pm B}. \quad (58)$$

Here the $K_{BB'}^{l^+ l^-, F\pm B}$ are leptonic factors given by

$$K_{BB'}^{l^+ l^-, F+B} = \frac{1}{3} (g_{vl} g'_{vl} + g_{al} g'_{al}) \left[\frac{3}{2} \frac{\mu^{4\varepsilon}}{2^{-2\varepsilon}} \frac{\pi^\varepsilon}{q^{2\varepsilon}} \frac{\Gamma(1-\varepsilon)}{\Gamma(1-2\varepsilon)} \frac{2-\varepsilon}{(3-2\varepsilon)(1-2\varepsilon)} \right], \quad (59)$$

$$K_{BB'}^{l^+ l^-, F-B} = \frac{1}{4} (g_{al} g'_{vl} + g_{vl} g'_{al}) \left[\frac{\mu^{4\varepsilon}}{2^{-2\varepsilon}} \frac{\pi^\varepsilon}{q^{2\varepsilon}} \frac{\Gamma(1-\varepsilon)}{\Gamma(1-2\varepsilon)} F(\varepsilon) \right]. \quad (60)$$

The factors in the square brackets are equal to $1 + \mathcal{O}(\varepsilon)$ and hence may be taken as 1 for calculational purposes, as they will always factorize exactly in next-to-leading order. Similarly, the Born term may be computed analogously in any valid n -dimensional regularization scheme. However, the Born term always factors out of the singular parts, which cancel (after mass factorization). Hence, the scheme dependence of the Born term cancels in the limit $\varepsilon \rightarrow 0$. This will be demonstrated explicitly in the following sections.

The F^{ab} are hadronic factors whose expressions are

$$F_{uu,BB'}^{q\bar{q},F+B} = -F_{ll,BB'}^{q\bar{q},F+B} = F_{uu,BB'}^{\bar{q}q,F+B} = -F_{ll,BB'}^{\bar{q}q,F+B} = g_{vq} g'_{vq} + g_{aq} g'_{aq}, \quad (61)$$

$$F_{ul,BB'}^{q\bar{q},F+B} = -F_{lu,BB'}^{q\bar{q},F+B} = F_{lu,BB'}^{\bar{q}q,F+B} = -F_{ul,BB'}^{\bar{q}q,F+B} = g_{aq} g'_{vq} + g_{vq} g'_{aq}, \quad (62)$$

and

$$F_{uu,BB'}^{q\bar{q},F-B} = -F_{ll,BB'}^{q\bar{q},F-B} = -F_{uu,BB'}^{\bar{q}q,F-B} = F_{ll,BB'}^{\bar{q}q,F-B} = g_{aq} g'_{vq} + g_{vq} g'_{aq}, \quad (63)$$

$$F_{ul,BB'}^{q\bar{q},F-B} = -F_{lu,BB'}^{q\bar{q},F-B} = -F_{lu,BB'}^{\bar{q}q,F-B} = F_{ul,BB'}^{\bar{q}q,F-B} = g_{vq} g'_{vq} + g_{aq} g'_{aq}. \quad (64)$$

V. VIRTUAL CORRECTIONS

The string of gamma matrices,

$$\gamma^\mu \gamma^\rho \gamma^\alpha (g_{vq} - g_{aq} \gamma_5) \gamma^\sigma \gamma_\mu, \quad (65)$$

arises in the calculation of the vertex graph (the massless self-energies vanish in n dimensions). In order to get the correct form for the virtual corrections, we must satisfy the relation,

$$\gamma^\mu \gamma^\rho \gamma^\alpha (g_{vq} - g_{aq} \gamma_5) \gamma^\sigma \gamma_\mu = \gamma^\mu \gamma^\rho \gamma^\alpha \gamma^\sigma \gamma_\mu (g_{vq} - g_{aq} \gamma_5), \quad (66)$$

which holds for an anticommuting γ_5 . The relation (66) is necessitated by the fact that the QED Ward identity [28] between vertex and self-energy graphs holds for the vector part. Therefore, we must be able to anticommute the γ_5 out of the vertex correction so that the axial-vector part factors correctly and the identity is trivially satisfied. In non-anticommuting- γ_5 schemes, this relation would be violated by terms of $\mathcal{O}(\varepsilon)$ (giving rise to a finite piece when multiplied by the $1/\varepsilon$ UV singularity) which would have to be removed by UV a counterterm analogous to that of DRED which corrects the γ - q vertex. Then, the result would be equivalent to that obtained using an anticommuting γ_5 in n dimensions, except that, in general, there could be additional terms of soft origin which must cancel when the bremsstrahlung contributions are added. If they did not cancel, the scheme would not be physically consistent since soft divergences cannot give rise to scheme dependences in physical cross sections.

It should be noted that we are assuming a vertex having the form (21). It was shown in [29] that using a symmetrized vertex can avoid the spurious UV terms, in the HVBM scheme, for the vertex $b \rightarrow s + H$. We investigated whether such a procedure would work here. Unfortunately, the situation is somewhat different than in $b \rightarrow s + H$. Considering, for simplicity, the case of W^\pm production, we find that the symmetrization procedure of [29] simply amounts to replacing the n -dimensional γ^α by the four-dimensional one. This clearly does not help remove the spurious UV terms; a counterterm will still be necessary. Of course, the ambiguity about whether to put the γ_5 on the right- or left-hand side of the γ^α is no longer present.

The string of gamma matrices (65) gets contracted with a tensor $I_{\rho\sigma}$ arising from the vertex loop integral. This is a good example to illustrate how the unphysical term arises in DRED. We will keep the argumentation general so that it is valid for both massless and massive quarks. Firstly, we have in DRED,

$$\gamma^\mu \gamma^\rho \gamma^\alpha \gamma^\sigma \gamma_\mu = -2\gamma^\sigma \gamma^\alpha \gamma^\rho. \quad (67)$$

$I_{\rho\sigma}$ has the form

$$I_{\rho\sigma} = g_{\rho\sigma}^n C_{24} + T_{\rho\sigma}, \quad (68)$$

where $T_{\rho\sigma}$ is a tensor which depends on the external momenta and C_{24} is a scalar coefficient. Performing the contraction gives

$$\begin{aligned} I_{\rho\sigma} \gamma^\sigma \gamma^\alpha \gamma^\rho &= \gamma^\sigma \gamma^\alpha \gamma^\rho g_{\rho\sigma}^n C_{24} + \gamma^\sigma \gamma^\alpha \gamma^\rho T_{\rho\sigma} \\ &= -2C_{24}[(1-\varepsilon)\gamma^\alpha + \gamma_\varepsilon^\alpha] + \gamma^\sigma \gamma^\alpha \gamma^\rho T_{\rho\sigma}, \end{aligned} \quad (69)$$

where we used the relation, valid for $n < 4$,

$$\gamma^\sigma \gamma^\alpha \gamma^\rho g_{\rho\sigma}^n = -2(1-\varepsilon)\gamma^\alpha - 2\gamma_\varepsilon^\alpha. \quad (70)$$

It is precisely the term $\sim \gamma_\varepsilon^\alpha$ which is removed by the DRED counterterm. The remaining terms give the correct result, i.e. that required to satisfy the QED Ward identity between vertex and self-energy graphs. That identity is most straightforwardly checked by retaining the quark mass, in order to avoid mass singularities. Having satisfied (66), the virtual corrections are analogous to those of the γ - q vertex, since the Born term simply factors out.

Using the Born term of the specific scheme, the net virtual contribution in a form valid for all consistent n -dimensional regularization schemes is ($ab = q\bar{q}, \bar{q}q$)

$$\begin{aligned} \left(\frac{d\hat{\sigma}_{mn, BB'}^{ab, F\pm B}}{dM} \right)_V &= \chi_{mn, BB'}^{ab, F\pm B}(\varepsilon) \delta(1-w) C_F \frac{\alpha_s}{2\pi} C(\varepsilon) \\ &\times \left[-\frac{2}{\varepsilon^2} - 7 + \frac{2\pi^2}{3} - \frac{2}{\varepsilon} \frac{P_{qq}^{n, \delta}}{C_F} \right], \end{aligned} \quad (71)$$

plus possible extra soft terms which would cancel with opposite ones in the soft bremsstrahlung, as discussed above. Here we defined

$$C(\varepsilon) \equiv \left(\frac{4\pi\mu^2}{M^2} \right)^\varepsilon \frac{\Gamma(1-\varepsilon)}{\Gamma(1-2\varepsilon)}. \quad (72)$$

The result (71) follows directly from that given in [4].

VI. BREMSSTRAHLUNG CORRECTIONS

The leptonic integrated $2 \rightarrow 3$ particle squared amplitudes have the form

$$\mathcal{M}_{mn, 2 \rightarrow 3}^{ab, F\pm B} = [c_F] \left(\frac{2\pi\alpha_s\mu^{2\varepsilon}}{M^2} \right) \tilde{\mathcal{M}}_{mn, 2 \rightarrow 2}^{ab, F\pm B} F_{mn, 2 \rightarrow 3}^{ab, F\pm B}, \quad (73)$$

where the factor c_F is present only for $ab = q\bar{q}, \bar{q}q$. The $\tilde{\mathcal{M}}$ are given by

$$\tilde{\mathcal{M}}_{mn,2\rightarrow 2}^{q\bar{q},F\pm B} = \tilde{\mathcal{M}}_{mn,2\rightarrow 2}^{qg,F\pm B} = \tilde{\mathcal{M}}_{mn,2\rightarrow 2}^{g\bar{q},F\pm B} = \mathcal{M}_{mn,2\rightarrow 2}^{q\bar{q},F\pm B} \quad (74)$$

and

$$\tilde{\mathcal{M}}_{mn,2\rightarrow 2}^{\bar{q}q,F\pm B} = \tilde{\mathcal{M}}_{mn,2\rightarrow 2}^{\bar{q}g,F\pm B} = \tilde{\mathcal{M}}_{mn,2\rightarrow 2}^{gq,F\pm B} = \mathcal{M}_{mn,2\rightarrow 2}^{\bar{q}q,F\pm B}. \quad (75)$$

For the qg subprocess in W^\pm production, the r.h.s. of (74), (75) implicitly contain a sum over the various quark flavors into which the gluon may split to form the W^\pm .

For the $q\bar{q}$ subprocess, we have

$$F_{mn}^{q\bar{q},F+B} = F_{mn}^{\bar{q}q,F+B} = \frac{s^2(1+w^2)}{p_1 \cdot k p_2 \cdot k} - 8, \quad (76)$$

$$F_{mn}^{q\bar{q},F-B} = F_{mn}^{\bar{q}q,F-B} = \frac{s^2(1+w^2)}{p_1 \cdot k p_2 \cdot k} - 4 \frac{s(1+w)}{p_1 \cdot q}. \quad (77)$$

For the qg subprocess, we have

$$F_{mn}^{(-)q/g/g^{(-)},F+B} = 2 \left[2w + 2 \frac{p_{2/1} \cdot k}{s} + s \frac{\Delta_{n/m} P_{qg}^4(w)}{p_{2/1} \cdot k} \right], \quad (78)$$

$$F_{mn}^{(-)q/g/g^{(-)},F-B} = 2 \left[s \frac{h_{mn}^{(-)q/g}(w)}{p_1 \cdot q} + 2w + 2 \frac{p_2 \cdot k}{s} + s \frac{\Delta_n P_{qg}^4(w)}{p_2 \cdot k} \right], \quad (79)$$

where

$$h_{uu/lu}^{(-)q/g} = -1 + w, \quad h_{ll/lu}^{(-)q/g} = 1 - w \quad (80)$$

and

$$F_{mn}^{g^{(-)q/g},F-B} = 2 \left[s \frac{h_{mn}^{g^{(-)q/g}}(w)}{p_1 \cdot q} - 2w - 2 \frac{p_1 \cdot k}{s} + s \frac{\Delta_m P_{qg}^4(w)}{p_1 \cdot k} \right], \quad (81)$$

with

$$h_{uu/ul}^{g^{(-)q/g}} = 2w^2, \quad h_{ll/lu}^{g^{(-)q/g}} = 2w. \quad (82)$$

Various checks on the above results are possible at this point. From crossing symmetry, it follows that

$$\mathcal{M}_{uu}^{qg,F\pm B} = -\frac{1}{2C_F} \mathcal{M}_{uu}^{q\bar{q},F\pm B}(p_2 \leftrightarrow -k), \quad \mathcal{M}_{uu}^{\bar{q}g,F\pm B} = -\frac{1}{2C_F} \mathcal{M}_{uu}^{\bar{q}q,F\pm B}(p_2 \leftrightarrow -k) \quad (83)$$

and

$$\mathcal{M}_{uu}^{gq,F+B} = -\frac{1}{2C_F} \mathcal{M}_{uu}^{\bar{q}q,F+B}(p_1 \leftrightarrow -k), \quad \mathcal{M}_{uu}^{g\bar{q},F+B} = -\frac{1}{2C_F} \mathcal{M}_{uu}^{q\bar{q},F+B}(p_1 \leftrightarrow -k). \quad (84)$$

The above correspondences were explicitly verified. (84) holds only for the $F+B$ case, since the $F-B$ integration depends on p_1 and hence destroys the crossing symmetry.

Also, the $q \leftrightarrow \bar{q}$ interchanges were checked using CPT invariance. The only difference between the $F-B$ and $F+B$ cases is that in the $F-B$ case, one picks up an extra minus under CPT, since CPT implies $l^+ \leftrightarrow l^-$ and the leptonic integration is antisymmetric.

The $2 \rightarrow 3$ particle bremsstrahlung phase space is given by

$$\left(\frac{d\hat{\sigma}_{mn,BB'}^{ab,F\pm B}}{dM} \right)_{\text{Br}} = \frac{2^{1+2\varepsilon}}{\pi^{1-\varepsilon}} M^{1-2\varepsilon} w^{1+\varepsilon} \frac{(1-w)^{1-2\varepsilon}}{\Gamma(1-\varepsilon)} \int_0^1 dy y^{-\varepsilon} (1-y)^{-\varepsilon} \int_{F\pm B} \mathcal{D}p_3 |M|_{mn,BB'}^{2ab}, \quad (85)$$

where

$$y = \frac{1 + \cos \theta}{2} \quad (86)$$

and θ is the angle between p_1 and k in the p_1, p_2 c.m..

Define

$$I_{mn}^{ab,F\pm B} \equiv \frac{(1-w)^{1-2\varepsilon}}{4} \frac{\Gamma(1-2\varepsilon)}{\Gamma^2(1-\varepsilon)} \int_0^1 dy y^{-\varepsilon} (1-y)^{-\varepsilon} F_{mn}^{ab,F\pm B}. \quad (87)$$

Then, noting (73), (57),

$$\left(\frac{d\hat{\sigma}_{mn,BB'}^{ab,F\pm B}}{dM} \right)_{\text{Br}} = [c_F] \frac{\alpha_s}{2\pi} \tilde{\chi}_{mn,BB'}^{ab,F\pm B}(\varepsilon) w^{1+\varepsilon} C(\varepsilon) I_{mn}^{ab,F\pm B}, \quad (88)$$

where the $\tilde{\chi}_{mn}^{ab,F\pm B}$ are defined analogously to the $\tilde{\mathcal{M}}_{mn}^{ab,F\pm B}$ (see (74), (75)). The resulting integrations are rather straightforward. Using the approach of [4] we may cast the $I_{mn}^{ab,F\pm B}$ in a form valid for all consistent n -dimensional regularization schemes, making use of the n -dimensional splitting functions $\Delta_k P_{ij}^n$. As for the virtual graphs, we omit a possible extra soft piece which would cancel in the virtual plus bremsstrahlung sum and use the Born term appropriate to the regularization scheme in question.

We obtain, for the $q\bar{q}$ subprocess,

$$I_{mn}^{q\bar{q},F\pm B} = \frac{2}{\varepsilon^2} \delta(1-w) - \frac{1}{\varepsilon} \frac{\Delta_{mn} P_{q\bar{q}}^{n,<}(w, \varepsilon)}{C_F} + 8 \left(\frac{\ln(1-w)}{1-w} \right)_+ - 4(1+w) \ln(1-w) + k_{mn}^{q\bar{q},F\pm B}(w), \quad (89)$$

with

$$k_{mn}^{q\bar{q},F+B}(w) = -2(1-w), \quad k_{mn}^{q\bar{q},F-B}(w) = 2(1+w) \ln w \quad (90)$$

and

$$\Delta_{mn} P_{ij} \equiv \Delta_m P_{ij} + \Delta_n P_{ij}. \quad (91)$$

For the qg subprocess, we obtain

$$I_{mn}^{ab,F\pm B} = -\frac{1}{\varepsilon} \Delta_{n/m}^{ab} P_{qg}^n(w) + 2 \ln(1-w) \Delta_{n/m}^{ab} P_{qg}^4(w) + k_{mn}^{ab,F\pm B}(w), \quad (92)$$

with

$$k_{mn}^{(\bar{q})q,F+B}(w) = k_{mn}^{g(\bar{q}),F+B}(w) = \frac{(1-w)}{4} (1+3w), \quad (93)$$

$$k_{uu,lu}^{(\bar{q})q,F-B}(w) = \frac{(1-w)}{4} (1+3w) + (1-w) \ln w, \quad (94)$$

$$k_{ll,ul}^{(\bar{q})q,F-B}(w) = \frac{(1-w)}{4} (1+3w) - (1-w) \ln w, \quad (95)$$

$$k_{uu,ul}^{g(\bar{q}),F-B}(w) = -\frac{(1-w)}{4} (1+3w) - 2w^2 \ln w, \quad (96)$$

$$k_{ll,lu}^{g(\bar{q}),F-B}(w) = -\frac{(1-w)}{4} (1+3w) - 2w \ln w \quad (97)$$

and

$$\Delta_{n/m}^{ab} P_{qg} \equiv \begin{cases} \Delta_n P_{qg} & : b = g \\ \Delta_m P_{qg} & : a = g \end{cases}. \quad (98)$$

VII. FACTORIZATION OF MASS SINGULARITIES

The term $\sim 1/\varepsilon^2$ in (89) represents a soft divergence (and simultaneous mass singularity) and is cancelled by an opposite term in (71). The remaining terms $\sim 1/\varepsilon$ in (71), (89), (92) represent mass singularities and do not cancel. Hence, they must be removed by expressing the bare parton distributions (and fragmentation functions in processes with final state mass singularities) in terms of the renormalized ones [30]. Thus, our parton model expression (18) is understood to be initially written in terms of the unrenormalized parton distributions, whose relation to the renormalized ones is given by

$$\begin{aligned} f_k^{0,i/A}(x, \mu^2) &= f_k^{r,i/A}(x, \mu^2) \\ &+ \frac{c(\varepsilon)}{\varepsilon} \sum_j \frac{\alpha_j}{2\pi} \int_x^1 \frac{dy}{y} f_k^{r,j/A}(y, \mu^2) \\ &\times [\Delta_k P_{ij}^4(x/y) + \varepsilon \Delta_k T_{ij}(x/y)], \end{aligned} \quad (99)$$

where

$$\frac{c(\varepsilon)}{\varepsilon} \equiv \frac{1}{\varepsilon}(4\pi)^\varepsilon \frac{\Gamma(1-\varepsilon)}{\Gamma(1-2\varepsilon)} = \frac{1}{\varepsilon} - \gamma_E + \ln 4\pi + \mathcal{O}(\varepsilon) \quad (100)$$

and $\alpha_j = \alpha_s$, unless $j (=A) = \gamma$, in which case $\alpha_j = \alpha$. After making the above substitution in (18), we recover the same form, except that now the subprocess cross section is finite and the parton distributions which enter are the renormalized (finite) ones. This will be demonstrated explicitly later. Note that photons, like hadrons, have internal partonic structure. Hence (99) is not restricted to hadronic initial states. We do not introduce the any additional mass scale here associated with the mass singularities as is commonly done. In this form, the above definition is consistent with the usual $\overline{\text{MS}}$ definition of renormalization when $\Delta_k T_{ij} = 0$, as will be discussed shortly.

The fragmentation functions $\mathcal{D}^{A/i}$, which represent the probability for quark i to split into a collinear hadron (or photon) A , with momentum fraction z , have the following renormalization:

$$\begin{aligned} \mathcal{D}_k^{0,A/i}(z, \mu^2) &= \mathcal{D}_k^{r,A/i}(z, \mu^2) \\ &+ \frac{c(\varepsilon)}{\varepsilon} \sum_j \frac{\alpha_j}{2\pi} \int_z^1 \frac{dy}{y} \mathcal{D}_k^{r,A/j}(y, \mu^2) \\ &\times [\Delta_k P_{ji}^4(z/y) + \varepsilon \Delta_k T_{ji}(z/y)]. \end{aligned} \quad (101)$$

All of the freedom in the factorization scheme is parametrized by the subtraction terms $T_{ij}(x/y)$. In theory, the T_{ij} could depend explicitly on x as well. Although we will discuss constraints on the allowed T_{ij} in some detail later in this section, it is worthwhile to briefly summarize the most commonly used schemes here. In Table I we list various schemes of interest. For the $\overline{\text{MS}}$ (as opposed to $\overline{\text{MS}}$) version of any of these schemes, simply add $(\gamma_E - \ln 4\pi)\Delta_k P_{ij}^4$ to the corresponding $\Delta_k T_{ij}$.

The ε modified minimal subtraction scheme ($\overline{\text{MS}}_\varepsilon$) was introduced in [4], the ‘polarized’ modified minimal subtraction scheme ($\overline{\text{MS}}_p$) was introduced in [25] and the ‘helicity conserving’ $\overline{\text{MS}}$ scheme ($\overline{\text{MS}}_{HC}$), as we shall refer to it, corresponds to the scheme used in determining the two-loop polarized splitting functions in [31]–[33], although it was inaccurately referred to as $\overline{\text{MS}}$ there and in many other papers making use of it. This inaccuracy appears to have been acknowledged in [33].

In HVBM regularization, the $\overline{\text{MS}}$ scheme leads to helicity nonconservation of massless fermions. Hence it is not generally used. The other three schemes are helicity conserving, at least in the direct sense. A potential problem in the $\overline{\text{MS}}_{HC}$ scheme will be discussed later in this section. For the $\overline{\text{MS}}_{HC}$ and $\overline{\text{MS}}_p$ schemes, one must use the $\overline{\text{MS}}$ scheme as the corresponding unpolarized factorization scheme when comparing polarized parton distributions to unpolarized ones. This is implicit in the definition of those two schemes, which are defined only for polarized parton distributions. This is an advantage since unpolarized parton distributions determined in the $\overline{\text{MS}}$ scheme are widely available, in contrast to the $\overline{\text{MS}}_\varepsilon$ scheme. On the other hand, it is not clear what effect these two schemes could have on various positivity constraints which require polarized quantities to be smaller in magnitude than the corresponding unpolarized ones, as will be discussed briefly at the end of this section. Nonetheless, presently available NLO polarized parton distributions are predominantly determined in the $\overline{\text{MS}}_{HC}$ scheme, so we will use it in making physical predictions.

The $\overline{\text{MS}}_\varepsilon$ scheme is the only of the three helicity conserving schemes with the following properties. **(a)** It treats the polarized and unpolarized parton distributions analogously. **(b)** It gives regularization scheme independent analytical results and parton distributions (equivalent to those of DRED $\overline{\text{MS}}$). **(c)** It satisfies the supersymmetric identity

$$\Delta_k P_{\tilde{g}\tilde{g}} + \Delta_k P_{g\tilde{g}} = \Delta_k P_{\tilde{g}g} + \Delta_k P_{gg}, \quad \tilde{g} = \text{gluino}, \quad (102)$$

for the unpolarized [34,35] and polarized [31,32] two-loop spacelike splitting functions as well as the timelike [33] splitting functions (both polarized and unpolarized). This is due to the equivalence with DRED, which in turn implies the applicability of four-dimensional calculational techniques. The timelike splitting functions are those which enter in (101). They only begin to differ from the spacelike ones at the two-loop level.

Substituting (99) in (18) and convoluting with the n -dimensional Born term of the regularization scheme being used generates several *factorization* counterterms. Those associated with the $q\bar{q}$ subprocess ($ab = q\bar{q}, \bar{q}q$) have the form

$$\left(\frac{d\hat{\sigma}_{mn,BB'}^{ab,F\pm B}}{dM} \right)_{\text{ct}} = \frac{1}{\varepsilon} \chi_{mn,BB'}^{ab,F\pm B}(\varepsilon) \frac{\alpha_s}{2\pi} w^{1+\varepsilon} C(\varepsilon) \left(\frac{s}{\mu^2} \right)^\varepsilon [\Delta_{mn} P_{q\bar{q}}^4(w) + \varepsilon \Delta_{mn} T_{q\bar{q}}(w)]. \quad (103)$$

The remaining terms are associated with the qg subprocess ($ab = \overset{(-)}{q} g, g \overset{(-)}{q}$) and have the form

$$\left(\frac{d\hat{\sigma}_{mn,BB'}^{ab,F\pm B}}{dM} \right)_{\text{ct}} = \frac{1}{\varepsilon} \tilde{\chi}_{mn,BB'}^{ab,F\pm B}(\varepsilon) \frac{\alpha_s}{2\pi} w^{1+\varepsilon} C(\varepsilon) \left(\frac{s}{\mu^2} \right)^\varepsilon [\Delta_{n/m}^{ab} P_{qg}^4(w) + \varepsilon \Delta_{n/m}^{ab} T_{qg}(w)]. \quad (104)$$

From [4] we may infer the relation between parton distributions of any regularization and factorization scheme, denoted 1, with any other, denoted 2:

$$f_{k,1}^{i/A}(x) = f_{k,2}^{i/A}(x) + \sum_j \frac{\alpha_j}{2\pi} \int_x^1 \frac{dy}{y} f_{k,2}^{j/A}(y) \{ [\Delta_k P_{1,ij}^\varepsilon(x/y) - \Delta_k T_{1,ij}(x/y)] - [\Delta_k P_{2,ij}^\varepsilon(x/y) - \Delta_k T_{2,ij}(x/y)] \} + \mathcal{O}(\alpha_j \alpha_s). \quad (105)$$

Similarly, for the fragmentation functions,

$$\mathcal{D}_{k,1}^{A/i}(z) = \mathcal{D}_{k,2}^{A/i}(z) + \sum_j \frac{\alpha_j}{2\pi} \int_z^1 \frac{dy}{y} \mathcal{D}_{k,2}^{A/j}(y) \{ [\Delta_k P_{1,ji}^\varepsilon(z/y) - \Delta_k T_{1,ji}(z/y)] - [\Delta_k P_{2,ji}^\varepsilon(z/y) - \Delta_k T_{2,ji}(z/y)] \} + \mathcal{O}(\alpha_j \alpha_s). \quad (106)$$

Going from scheme 1 to scheme 2 simply amounts to expressing the parton distributions and fragmentation functions of scheme 1 in terms of those of scheme 2, as was shown in [4]. Also, we see that working in any consistent n -dimensional regularization scheme and any factorization scheme is equivalent to working in any other consistent n -dimensional regularization scheme with the appropriate factorization scheme. Thus, according to our definition of consistency given in section III, a consistent n -dimensional regularization scheme must (a) be mathematically consistent, for the class of subprocesses under consideration, and (b) have a process independent set of splitting functions within that class, in order that it may be related to the HVBM scheme as described in section III (assuming DREG and HVBM themselves do not fail for some process, unlikely as it may seem). The DRED scheme satisfies both criteria for one-loop QCD corrections to polarized processes.

From [4] we may also infer that the conversion term which must be added to the subprocess cross section calculated in scheme 1 to obtain the subprocess cross section in scheme 2 is obtained via

$$\hat{\sigma}_{conv} = \sum_l \hat{\sigma}_{ct,l} \{ [\Delta_k P_{ij}^4(w_l) + \varepsilon \Delta_k T_{1,ij}(w_l)] \rightarrow \varepsilon [\Delta_k T_{2,ij}(w_l) - \Delta_k P_{2,ij}^\varepsilon(w_l)] - \varepsilon [\Delta_k T_{1,ij}(w_l) - \Delta_k P_{1,ij}^\varepsilon(w_l)] \}, \quad (107)$$

where w_l is the argument of the splitting functions in the counterterm $\hat{\sigma}_{ct,l}$. The conversion terms are generated by making the above substitution in all factorization counterterms for both initial and final state mass singularities in general. As well, one must express the couplings of scheme 1 in terms of those in scheme 2 for processes where coupling constant renormalization enters. Then, the above form is valid for all one-loop QCD corrections, not just Drell-Yan and DIS. Also, it is straightforward to verify that making the substitutions (105), (106) in any one-loop cross section calculated in scheme 1, leads to the conversion term (107).

Parton distributions determined using different processes, but the same scheme, will differ by $\mathcal{O}(\alpha_s^{n+1})$ when $\mathcal{O}(\alpha_s^n)$ corrected cross sections are used in the fits. Since a basic assumption of the parton model is that the all-orders parton distributions will be process independent, the process dependence of the parton distributions can be seen to arise from the neglected higher orders. The physical parton distributions are in fact the all-orders parton distributions since, in reality, it is the all-orders subprocess cross section that they are convoluted with. Hence, if the all-orders parton distributions were not process independent, there would exist no process independent parton distributions. By all orders, we mean sufficiently high order in α_s that higher orders may be neglected for all practical purposes. The process dependence is therefore easy to understand since some processes have large QCD corrections (i.e. Drell-Yan) while others have relatively small corrections (i.e. DIS). Hence the extent to which the $\mathcal{O}(\alpha_s^n)$ and $\mathcal{O}(\alpha_s^{n+1})$ parton distributions differ, in any particular scheme, will depend on the process from which they are determined. So, for low n (i.e. $n = 0$), processes with significantly different QCD corrections will yield somewhat different parton distributions, but the ones with smaller QCD corrections will lead to parton distributions which are closer to the all-orders ones. One expects, on the other hand, that the ratio of the polarized to unpolarized parton distributions will not have a large process dependence since, even for Drell-Yan like processes, spin asymmetries tend to exhibit perturbative stability as we shall demonstrate in sections IX – XI.

Equation (105) is very powerful and restrictive. This is because it has implications for various conservation rule motivated sum rules. According to the parton model, the number of valence (constituent) quarks, q_v , in a hadron, A , is given by

$$N^{q_v/A} = \int_0^1 dy f_u^{q_v/A}(y) = \text{const.} \quad (108)$$

More specifically,

$$\begin{aligned} N^{d_v/p} &= N^{d/p} - N^{\bar{d}/p} = 1, \\ N^{u_v/p} &= N^{u/p} - N^{\bar{u}/p} = 2. \end{aligned} \quad (109)$$

The fact that this must hold for all energy scales, μ , is an expression of charge/probability conservation. Since $N^{q/A}$ is just the first moment of $f_u^{q/A}(y)$ and since the k^{th} moment of a convolution is the product of the k^{th} moments of the functions being convoluted, it is easy to see what happens to the above conserved quantity as one goes from one scheme to another.

Firstly, we note that the gluonic contribution of (105) to the relation between quark distributions of different schemes cancels for the valence distributions. Suppose we wish to see what happens when going from regularization scheme 2 to regularization scheme 1. Using (105), we get, for valence quarks,

$$N_1^{qv/A} = N_2^{qv/A} \left\{ 1 + \frac{\alpha_s}{2\pi} [(\Delta_u \bar{P}_{1,qq}^\varepsilon - \Delta_u \bar{T}_{1,qq}) - (\Delta_u \bar{P}_{2,qq}^\varepsilon - \Delta_u \bar{T}_{2,qq})] \right\}, \quad (110)$$

where \bar{g} denotes the first moment of $g(y)$, for some function g . Suppose scheme 1 is DRED, for which $\Delta_u P_{DRED,qq}^\varepsilon = 0$, and scheme 2 is DREG, for which

$$\Delta_u \bar{P}_{DREG,qq}^\varepsilon = 0, \quad (111)$$

as can be seen from (29). Assuming the same factorization scheme, i.e. $\Delta_u T_{2,ij} = \Delta_u T_{1,ij}$, we obtain

$$N_{DRED}^{qv/A} = N_{DREG}^{qv/A}, \quad (112)$$

so that the two regularization schemes are mutually physically consistent regarding charge conservation. The requirement,

$$\Delta_u \bar{P}_{qq}^n = 0, \quad (113)$$

follows from the fact that the $\mathcal{O}(\alpha_s)$ corrections to charge conservation must be zero in n dimensions. By corrections, we mean that one can think of a zeroth order piece to $\Delta_u P_{qq}(z)$, $\Delta_u P_{gg}(z)$ which is proportional to $\delta(1-z)$ and denotes the no interaction scenario. Then, it is clear that the usual leading order splitting functions denote $\mathcal{O}(\alpha_s)$ corrections to the non-interacting case.

Let us now consider momentum conservation. Let $P^{i/A}$ denote the total momentum fraction carried by parton i . It is just the second moment of $f_u^{i/A}$:

$$P^{i/A} = \int_0^1 dy y f_u^{i/A}(y). \quad (114)$$

Of course, momentum conservation must be applied to the sum over all partons. One can easily verify that if, in some factorization scheme, the DRED parton distributions satisfy the momentum conservation rule

$$\sum_i P^{i/A} = 1, \quad (115)$$

then the DREG parton distributions, in that same factorization scheme, will also satisfy it, and vice-versa. The basic reason is that the requirement, which DREG satisfies, that

$$\begin{aligned} & \int_0^1 dz z [\Delta_u P_{qq}^n(z) + \Delta_u P_{gg}^n(z)] \\ &= \int_0^1 dz z [\Delta_u P_{gg}^n(z) + 2N_F \Delta_u P_{qq}^n(z)] = 0, \end{aligned} \quad (116)$$

(which follows from the fact that the $\mathcal{O}(\alpha_s)$ corrections to momentum conservation must be zero, in n dimensions) leads to cancellations in the sum over partons, so that the net difference in total momentum between schemes is zero. This is easily verified from Eq. (29). The individual quark and gluon momentum fractions will depend on the regularization (and factorization) scheme as well as the energy scale, μ , to $\mathcal{O}(\alpha_s)$, but a change in the quark momentum fraction is cancelled by an exactly opposite change in the gluon momentum fraction. Thus, the total momentum is the same in both schemes, and is independent of μ , as follows from DGLAP evolution [36,23].

All this discussion tells us that DRED and DREG are mutually physically consistent in general, in the unpolarized case. One can convert unpolarized parton densities from one regularization scheme to the other and the conserved quantities retain their values. The real problem arises when one converts from one factorization scheme to another. It is safe to go from $\overline{\text{MS}}$ to MS since, in the MS scheme, all the $\Delta_k T_{ij}$ are proportional to $\Delta_k P_{ij}^A(\gamma_E - \ln 4\pi)$, and hence do not change the conserved quantities. Also, since DRED is equivalent to the $\overline{\text{MS}}_\varepsilon$ scheme, we see that $\overline{\text{MS}}_\varepsilon$ and $\overline{\text{MS}}$ are mutually physically consistent as well, for unpolarized processes. In general though, for arbitrary $\Delta_k T_{ij}$, there are no analogous constraints to (113) and (116), at least without invoking constraints from higher order evolution. This means that the aforementioned conserved quantities will differ in general to $\mathcal{O}(\alpha_s)$ when going from one arbitrarily chosen factorization scheme to another. Since it would be quite

a formidable task to measure so precisely the parton distributions that one could definitely verify all conserved quantities to high accuracy, how do we know which schemes are correct a-priori? This is even more pertinent to the case of the polarized parton distributions, where the data is definitely lacking.

We may gain some insight into this issue by studying the scheme dependence of the polarized (nonsinglet) distributions. The net spin, $S^{q/A}$, carried by quarks of flavor q , in hadron A , and the corresponding total quark spin, $\frac{1}{2}\Delta\Sigma_A$, are given by

$$S^{q/A} = \frac{1}{2} \int_0^1 dy f_l^{q/A}(y), \quad \frac{1}{2}\Delta\Sigma_A = \sum_q S^{q/A}, \quad (117)$$

respectively. The spin carried by the valence quarks is conserved under one-loop evolution due to chirality conservation. More formally, $\Delta_l \bar{P}_{qq}^4 = 0$, substituted in the expression for the first moment of $f_l^{q/A}$, evolved using the DGLAP equations gives $S^{q_v/A} = \text{const}$, under one-loop evolution, as was the case for $N^{q_v/A}$. For a discussion of two-loop valence evolution effects, which in general violate the above conservation, the reader is referred to [37]. The main point of interest concerning two-loop evolution is that chirality conservation is relevant to nonsinglet combinations of the form $f_l^q + f_l^{\bar{q}} - f_l^{q'} - f_l^{\bar{q}'}$, and linear combinations thereof. The two interesting ones ΔA_3 , ΔA_8 satisfy

$$\Delta \bar{A}_{3,8} = \text{const}, \quad (118)$$

where

$$\begin{aligned} \Delta A_3 &= f_l^u + f_l^{\bar{u}} - f_l^d - f_l^{\bar{d}} \\ \Delta A_8 &= f_l^u + f_l^{\bar{u}} + f_l^d + f_l^{\bar{d}} - 2(f_l^s + f_l^{\bar{s}}). \end{aligned} \quad (119)$$

Similar argumentation to that used in relating $N_1^{q_v/A}$ to $N_2^{q_v/A}$ leads to

$$\begin{aligned} \Delta \bar{A}_{3,8}^1 &= \Delta \bar{A}_{3,8}^2 \left\{ 1 + \frac{\alpha_s}{2\pi} [(\Delta_l \bar{P}_{1,qq}^\varepsilon - \Delta_l \bar{T}_{1,qq}) \right. \\ &\quad \left. - (\Delta_l \bar{P}_{2,qq}^\varepsilon - \Delta_l \bar{T}_{2,qq})] \right\}, \end{aligned} \quad (120)$$

From Table I and Eq. (30) we get

$$\begin{aligned} \Delta \bar{A}_{3,8}^{DRED(\overline{\text{MS}})} &= \Delta \bar{A}_{3,8}^{HV(\overline{\text{MS}}_\varepsilon)} = \Delta \bar{A}_{3,8}^{HV(\overline{\text{MS}}_{HC})} \\ &= \Delta \bar{A}_{3,8}^{HV(\overline{\text{MS}}_p)} \neq \Delta \bar{A}_{3,8}^{HV(\overline{\text{MS}})}. \end{aligned} \quad (121)$$

Thus, the $\overline{\text{MS}}$ scheme of DREG(HVBM) gives different values for $\Delta \bar{A}_3$, $\Delta \bar{A}_8$ than all the ‘chirality conserving’ schemes. This is an explicit example of the factorization scheme ambiguity.

The real implication of this seeming nonuniqueness problem is that certain factorization schemes may be ruled out from the beginning since they are manifestly unphysical. One can determine which schemes are unphysical by imposing the fact that the unrenormalized parton distributions (99) themselves satisfy the conservation rules (108), (115) and (118) and yield the correct value for the corresponding conserved quantities (except as will be mentioned below). The reason for this is that if a particular regularization preserves the necessary symmetries: unitarity, translation invariance and chiral symmetry, then the unrenormalized parton distributions in that regularization will obey the corresponding conservation rules: conservation of charge/probability, momentum, and massless quark chirality. Hence, the connection between renormalized and unrenormalized parton distributions must not destroy those symmetries in the renormalized parton distributions. If, on the other hand, a regularization violates a particular symmetry, a finite $\Delta_k T_{ij}$ will have to be introduced to insure that the renormalized parton distributions obey the corresponding conservation rule, since the unrenormalized parton distributions themselves will manifestly violate it.

Thus, using similar rationale to that used in going from one regularization scheme to another, we arrive at the physical consistency constraints on allowable factorization schemes,

$$\int_0^1 dz \Delta_u T_{qq}(z) = 0, \quad (122)$$

$$\begin{aligned} &\int_0^1 dz z [\Delta_u T_{qq}(z) + \Delta_u T_{gq}(z)] \\ &= \int_0^1 dz z [\Delta_u T_{gg}(z) + 2N_F \Delta_u T_{qg}(z)] = 0 \end{aligned} \quad (123)$$

and

$$\Delta_l T_{qq}(z) - \Delta_l P_{qq}^\varepsilon(z) = \Delta_u T_{qq}(z) - \Delta_u P_{qq}^\varepsilon(z). \quad (124)$$

The reason we had to subtract $\Delta_k P_{qq}^\varepsilon$ in (124) is that for regularization schemes like HVBM which violate chiral symmetry ($\Delta_l P_{qq}^\varepsilon \neq \Delta_u P_{qq}^\varepsilon$), the unrenormalized parton distributions themselves manifestly violate helicity conservation. One must always subtract the helicity nonconserving part in $\Delta_l P_{qq}^\varepsilon$ in order to restore this conservation. This is why HVBM($\overline{\text{MS}}$) disagrees with the other schemes and is manifestly unphysical. Under two-loop evolution, helicity non-conservation in HVBM($\overline{\text{MS}}$) manifests itself via direct violation of (118). This may be seen by taking scheme 1 to be HVBM($\overline{\text{MS}}$) and scheme 2 to be one of the ‘chirality conserving’ schemes, then differentiating (120) with respect to $\ln \mu^2$. Comparing with the DGLAP equation for $\Delta \overline{A}_{3,8}^1$ one finds precisely the same nonvanishing result for $d\Delta \overline{A}_{3,8}^1/d\ln \mu^2$ as follows from the two-loop analysis [31,32].

The condition (124) is somewhat stronger than the conservation rule (118). It also insures that

$$\hat{\sigma}(\text{helicity flip}) = 0, \quad (125)$$

where $\hat{\sigma}(\text{helicity flip})$ generically denotes any doubly polarized (in the initial state) subprocess cross section where a massless quark flips helicity, with the helicity at both ends of the quark line fixed.

The relation between the total quark spin in scheme 1 and that in scheme 2 is obtained by taking the first moment of (105) and summing over quarks (including antiquarks),

$$\begin{aligned} \frac{1}{2}\Delta\Sigma_1 = \frac{1}{2}\Delta\Sigma_2 + \frac{\alpha_s}{4\pi} \left\{ \sum_q \bar{f}_l^q [(\Delta_l \overline{P}_{1,qq}^\varepsilon - \Delta_l \overline{T}_{1,qq}) - (\Delta_l \overline{P}_{2,qq}^\varepsilon - \Delta_l \overline{T}_{2,qq})] \right. \\ \left. + 2N_f \bar{f}_l^g [(\Delta_l \overline{P}_{1,qg}^\varepsilon - \Delta_l \overline{T}_{1,qg}) - (\Delta_l \overline{P}_{2,qg}^\varepsilon - \Delta_l \overline{T}_{2,qg})] \right\}. \end{aligned} \quad (126)$$

Since DRED preserves chiral symmetry, it is natural to use it as a reference scheme. If we also desire that the total spin of the quarks be the same as in DRED($\overline{\text{MS}}$), then $\Delta_l \overline{P}_{qq}^\varepsilon \neq 0$ in HVBM regularization leads to violation of this in the $\overline{\text{MS}}_{HC}$ scheme. We must impose

$$\int_0^1 dz [\Delta_l T_{qq}(z) - \Delta_l P_{qq}^\varepsilon(z)] = 0 \quad (127)$$

to restore equivalence. Hence, of the factorization schemes listed in Table I, only $\overline{\text{MS}}_\varepsilon$ and $\overline{\text{MS}}_p$ give the value of total quark spin equal to that in DRED($\overline{\text{MS}}$).

One may ask if there is some deeper physical reason why the $\overline{\text{MS}}_{HC}$ scheme gives a different value for the total quark spin. We notice, using (29) and (30), that in the HVBM scheme

$$P_{qq,++}^n(z) \neq P_{qq,-+}^n(1-z). \quad (128)$$

This means that when a polarized gluon splits into a collinear $q\bar{q}$ pair, the q and \bar{q} do not necessarily have opposite chiralities, as required by quark chirality conservation. The above result is possible since, if there is an initial state gluon, (125) does not apply.

The $\overline{\text{MS}}_\varepsilon$ and $\overline{\text{MS}}_p$ schemes correct (128), while $\overline{\text{MS}}_{HC}$ does not. More precisely, strictly speaking, chirality conservation imposes the indirect constraint,

$$\begin{aligned} & [\Delta_u T_{qq}(z) + \Delta_l T_{qq}(z)] - [\Delta_u P_{qq}^\varepsilon(z) + \Delta_l P_{qq}^\varepsilon(z)] \\ &= [\Delta_u T_{qq}(1-z) - \Delta_l T_{qq}(1-z)] - [\Delta_u P_{qq}^\varepsilon(1-z) - \Delta_l P_{qq}^\varepsilon(1-z)] \\ &\Rightarrow \Delta_l T_{qq}(z) - \Delta_l P_{qq}^\varepsilon(z) = -[\Delta_l T_{qq}(1-z) - \Delta_l P_{qq}^\varepsilon(1-z)], \end{aligned} \quad (129)$$

which both $\overline{\text{MS}}_\varepsilon$ and $\overline{\text{MS}}_p$ satisfy, but $\overline{\text{MS}}_{HC}$ does not. The reason, as usual, is that it is the difference, $\Delta_k P_{ij}^\varepsilon(z) - \Delta_k T_{ij}(z)$, which enters in physical cross sections. Thus, the subtraction term, $\Delta_k P_{ij}^\varepsilon(z)$, effectively modifies the splitting function, $\Delta_k T_{ij}(z)$. The unpolarized parts in (129) cancelled due to the unpolarized constraint, $\Delta_u T_{qq}(z) - \Delta_u P_{qq}^\varepsilon(z) = \Delta_u T_{qq}(1-z) - \Delta_u P_{qq}^\varepsilon(1-z)$, which is satisfied in all the schemes considered here. Satisfaction of (129) implies satisfaction of (127), while the reverse is not true. An interesting analysis which arrived, from a different perspective, at a conclusion similar to (127), in the context of DIS, may be found in [38]. How strictly one wishes to impose chirality conservation is perhaps a matter of taste, however.

Under one-loop evolution, the total quark spin is conserved. Under two-loop evolution, conservation or non-conservation depends on the choice of factorization scheme. Analogously to the nonsinglet case, we see that if $\Delta\Sigma_2$ is conserved and $\Delta\Sigma_1 \neq \Delta\Sigma_2$, then $\Delta\Sigma_1$ will not be conserved under two-loop evolution. The scale dependence of $\Delta\Sigma_1$ may be obtained by differentiating (126) directly. The $\overline{\text{MS}}_\varepsilon$ and $\overline{\text{MS}}_p$ schemes lead to conservation of $\Delta\Sigma$, therefore $\overline{\text{MS}}_{HC}$ does not. Alternatively worded, $\Delta\Sigma$ is not conserved in the $\overline{\text{MS}}_{HC}$ scheme and the difference in the schemes exactly compensates this non-conservation such that $\Delta\Sigma$ is conserved in the $\overline{\text{MS}}_\varepsilon$ and $\overline{\text{MS}}_p$ schemes. The evolution of $\Delta\Sigma$ in the $\overline{\text{MS}}_{HC}$ scheme obtained via differentiation of (126) agrees with the two-loop analysis [31,32] and can be seen to arise from the non-vanishing of $\Delta_l \overline{P}_{qq}^\varepsilon$. Under two-loop evolution, it is the non-vanishing

of the first moment of $\Delta_L P_{qq}$ (from the pure singlet part) which leads to the non-conservation of $\Delta\Sigma$, however. Hence the non-vanishing at two-loops of $\Delta_L \bar{P}_{qq}$ is seen to be a consequence of the non-vanishing at one-loop of $\Delta_L \bar{P}_{qq}^\varepsilon$, while $\Delta_L \bar{P}_{qg}$ remains zero at two loops, in all three schemes.

At any rate, we see that satisfaction of (127) leads to conservation of total quark spin. The DGLAP evolution equations will be elaborated on in the next section in connection with scale dependences. It is worth noting that analogous argumentation can be used to relate the spin carried by the gluons in different schemes. Since such differences do not enter in the observables considered here, at one loop, we will not discuss them. Also, direct differentiation of (105) gives the correct scheme transformations for all two-loop splitting functions, generalized to include the regularization scheme dependence (i.e. $T_{ij} \rightarrow T_{ij} - P_{ij}^\varepsilon$).

So far, we have not discussed the interesting requirement of positivity of the parton distributions,

$$f_{+/+}^{i/I}(x, \mu^2) \geq 0, \quad f_{-/+}^{i/I}(x, \mu^2) \geq 0. \quad (130)$$

The only guarantee of positivity applies to the physical cross section itself, as measured by experiment. Individual subprocess cross sections need not satisfy positivity due to the interconnection of the subprocesses arising from the renormalization of the parton distributions discussed earlier in this section. To the extent that leading order cross sections dominate and that the parton distributions are process independent at leading order, positivity should not be a problem. On the other hand, for processes with large radiative corrections, some factorization schemes could lead to parton distributions in violation of (130). This issue has not been thoroughly studied at this point, but it will become important as more experiments involving polarized hadrons are undertaken.

VIII. ANALYTICAL RESULTS TO ONE-LOOP ORDER

We may now present the analytical results for $d\hat{\sigma}_{mn, BB'}^{ab, F\pm B}/dM$ in a form valid for all consistent n -dimensional regularization schemes and for a general factorization scheme, starting with the $q\bar{q}$ subprocess. Combining (57), (71), (88), (89) and (103), we obtain the total result ($ab = q\bar{q}, \bar{q}q$),

$$\begin{aligned} \left(\frac{d\hat{\sigma}_{mn, BB'}^{ab, F\pm B}}{dM} \right)_{\text{NLO}} &= \chi_{mn, BB'}^{ab, F\pm B}(0) \left(\delta(1-w) + C_F \frac{\alpha_s}{2\pi} w \left\{ \left(\frac{2\pi^2}{3} - 7 \right) \delta(1-w) \right. \right. \\ &\quad + 8 \left(\frac{\ln(1-w)}{1-w} \right)_+ + \frac{\Delta_{mn} P_{q\bar{q}}^4(w)}{C_F} \ln \frac{M^2}{w\mu^2} - 4(1+w) \ln(1-w) \\ &\quad \left. \left. + \frac{1}{C_F} [\Delta_{mn} T_{q\bar{q}}(w) - \Delta_{mn} P_{q\bar{q}}^\varepsilon(w)] + k_{mn}^{q\bar{q}, F\pm B}(w) \right\} \right), \end{aligned} \quad (131)$$

where the $k_{mn}^{q\bar{q}, F\pm B}$ are given in (90).

We now present the result for the qg subprocess. There is no $\mathcal{O}(1)$ term (in α_s). Combining (88), (92) and (104), we obtain the total result ($ab = \overset{(-)}{q} g, g \overset{(-)}{q}$),

$$\begin{aligned} \left(\frac{d\hat{\sigma}_{mn, BB'}^{ab, F\pm B}}{dM} \right)_{\text{NLO}} &= \tilde{\chi}_{mn, BB'}^{ab, F\pm B}(0) \frac{\alpha_s}{2\pi} w \left\{ \Delta_{n/m}^{ab} P_{qg}^4(w) \left[\ln \frac{M^2}{w\mu^2} + 2 \ln(1-w) \right] \right. \\ &\quad \left. + [\Delta_{n/m}^{ab} T_{qg}(w) - \Delta_{n/m}^{ab} P_{qg}^\varepsilon(w)] + k_{mn}^{ab, F\pm B}(w) \right\}, \end{aligned} \quad (132)$$

where the $k_{mn}^{ab, F\pm B}(w)$ are given by (93) – (97).

We see at this point that the results of [4] (for the uu and ll , $F+B$, vector coupling case with massless $B=B'$) are contained within the results presented here. Those, in turn, were found to be consistent with various existing results calculated in certain specific schemes, for both the uu [39,40] and ll [1,2] cases. Single-spin W^\pm production in hadron-hadron collisions has been studied in [3]. Considering the subprocess $ab \rightarrow W^\pm c$, where a is longitudinally polarized and b is unpolarized, we see that for $ab = q\bar{q}, \bar{q}q$ and for $a = g, b = \overset{(-)}{q}$, our expressions reproduce those given in Appendix B of [3]. For $a = \overset{(-)}{q}, b = g$, it seems at first sight that there is a discrepancy. In order to reproduce the result of [3], one needs $\Delta_u P_{qg}^\varepsilon = -1/2$, in disagreement with (29). The reason for this disagreement is that [3] averages over 2, rather than $2-2\varepsilon$, gluon polarization states, as can be inferred from their Eq. (10). That convention does indeed lead to $\Delta_u P_{qg}^\varepsilon = -1/2$. Unfortunately, all of the presently available unpolarized parton distributions are determined using the convention of $2-2\varepsilon$ gluon polarization states. Consequently, the expressions of [3], for the qg subprocess, should be appropriately converted using the technique of [4], which amounts to Eq. (107) of this paper, before being used in numerical studies demanding complete consistency at NLO.

At this point, we may investigate the scale dependence of the cross section. Define

$$\sigma \equiv \frac{d\sigma_{mn}^{AB,F\pm B}}{dM} \quad (133)$$

and let $\tilde{\sigma}$ denote the contribution to σ which depends on μ^2 at $\mathcal{O}(\alpha_s)$ coming from $a = q$, $b = \bar{q}$; $a = q$, $b = g$ and $a = g$, $b = \bar{q}$ for one quark flavor and for production by one bosonic interference channel. These subprocesses are connected via the renormalization of the parton distributions, but are disconnected from the remaining subprocesses in that sense. We have (taking $\mathcal{S}_m^A = \mathcal{S}_n^B = 1$)

$$\begin{aligned} \tilde{\sigma} = \chi_{mn}^{q\bar{q},F\pm B}(0) & \left\{ \int_{\tau}^1 dx_{a,b} \int_{\tau/x_{a,b}}^1 dx_{b,a} f_m^q(x_a, \mu^2) f_n^{\bar{q}}(x_b, \mu^2) \delta(1 - \frac{\tau}{x_a x_b}) \right. \\ & - \frac{\alpha_s}{2\pi} \int_{\tau}^1 dx_b \frac{\tau}{x_b} f_n^{\bar{q}}(x_b, \mu^2) \int_{\tau/x_b}^1 \frac{dx_a}{x_a} [f_m^q(x_a, \mu^2) \Delta_m P_{qq}^4(w) \ln \mu^2 + f_m^g(x_a, \mu^2) \Delta_m P_{qg}^4(w) \ln \mu^2] \\ & \left. - \frac{\alpha_s}{2\pi} \int_{\tau}^1 dx_a \frac{\tau}{x_a} f_m^q(x_a, \mu^2) \int_{\tau/x_a}^1 \frac{dx_b}{x_b} [f_n^{\bar{q}}(x_b, \mu^2) \Delta_n P_{qq}^4(w) \ln \mu^2 + f_n^g(x_b, \mu^2) \Delta_n P_{qg}^4(w) \ln \mu^2] \right\}, \end{aligned} \quad (134)$$

where

$$f_k^j(x_{a,b}, \mu^2) \equiv f_k^{j/A,B}(x_{a,b}, \mu^2). \quad (135)$$

In DIS, one has an analogous expression, except without the convolution with the $f_n^{\bar{q}}$ term. The independence of σ on μ to $\mathcal{O}(\alpha_s)$ implies

$$\frac{d\tilde{\sigma}}{d \ln \mu^2} = \mathcal{O}(\alpha_s^2). \quad (136)$$

Here we note

$$\frac{d\alpha_s}{d \ln \mu^2} = -\frac{\beta_0}{4\pi} \alpha_s^2 = \mathcal{O}(\alpha_s^2). \quad (137)$$

Taking into account the fact that the evolution of $f_m^{q/A}$ is independent of $f_n^{\bar{q}/B}$ and $f_n^{g/B}$, we may arbitrarily set, for any fixed μ^2 , $f_n^g(x_b, \mu^2) = 0$ and $f_n^{\bar{q}}(x_b, \mu^2) = \delta(1 - x_b)$, after performing the differentiation in (136). Of course, $f_n^{g/B}$ and $f_n^{\bar{q}/B}$ still evolve with μ^2 . We then use (136) with $m = n$, $f_n^g(x_a, \mu^2) = f_n^g(x_b, \mu^2) = 0$ and $f_n^q(x_a, \mu^2) = \delta(1 - x_a)$, $f_n^{\bar{q}}(x_b, \mu^2) = \delta(1 - x_b)$ to solve for and eliminate $df_n^{\bar{q}}(x_b, \mu^2)/d \ln \mu^2$. The result for $df_n^{\bar{q}}(x_b, \mu^2)/d \ln \mu^2$ is simply $\frac{\alpha_s}{2\pi} \Delta_n P_{qq}^4(x_b)$.

We thus obtain

$$\frac{df_k^q(x, \mu^2)}{d \ln \mu^2} = \frac{\alpha_s(\mu^2)}{2\pi} \int_x^1 \frac{dy}{y} [f_k^q(y, \mu^2) \Delta_k P_{qq}^4(x/y) + f_k^g(y, \mu^2) \Delta_k P_{qg}^4(x/y)] + \mathcal{O}(\alpha_s^2), \quad (138)$$

for $k = u, l$. This is the DGLAP equation [36,23] with one-loop splitting functions. Therefore, one needs at least one-loop evolution to guarantee μ^2 independence to $\mathcal{O}(\alpha_s)$. Gluonic evolution only enters at the $\mathcal{O}(\alpha_s^2)$ level.

We may write, using the Taylor expansion for fixed x ,

$$\begin{aligned} f_k^q(x, \mu^2) &= f_k^q(x, \mu_0^2) + \frac{\alpha_s(\mu_0^2)}{2\pi} \ln \left(\frac{\mu^2}{\mu_0^2} \right) c_{1,k}^q(x, \mu_0^2) + \left[\frac{\alpha_s(\mu_0^2)}{2\pi} \ln \left(\frac{\mu^2}{\mu_0^2} \right) \right]^2 c_{2,k}^q(x, \mu_0^2) + \dots \\ &\equiv f_k^q(x, \mu_0^2) + \frac{\alpha_s(\mu_0^2)}{2\pi} \ln \left(\frac{\mu^2}{\mu_0^2} \right) c_{1,k}^q(x, \mu_0^2) \\ &\quad + \left[\frac{\alpha_s(\mu_0^2)}{2\pi} \ln \left(\frac{\mu^2}{\mu_0^2} \right) \right]^2 \tilde{f}_k^q(x, \mu^2, \mu_0^2), \end{aligned} \quad (139)$$

where

$$c_{1,k}^q(x, \mu_0^2) = \int_x^1 \frac{dy}{y} [f_k^q(y, \mu_0^2) \Delta_k P_{qq}^4(x/y) + f_k^g(y, \mu_0^2) \Delta_k P_{qg}^4(x/y)]. \quad (140)$$

One can write an analogous expression for $f_k^g(x, \mu^2)$ using the DGLAP evolution equation for $f_k^g(x, \mu^2)$, yielding

$$c_{1,k}^g(x, \mu_0^2) = \int_x^1 \frac{dy}{y} \left[\sum_{i=1}^{2N_f} f_k^{qi}(y, \mu_0^2) \Delta_k P_{qg}^4(x/y) + f_k^g(y, \mu_0^2) \Delta_k P_{gg}^4(x/y) \right]. \quad (141)$$

Then one could express σ in terms of the \tilde{f} and parametrize explicitly the $\mathcal{O}(\alpha_s^2) \mu^2$ dependence with respect to some fixed scale μ_0^2 . Suppose μ_0^2 is a typical scale of the process (i.e. M^2), then there will not be any large logarithms and $\sigma(\mu_0^2)$ will have reasonable $\mathcal{O}(\alpha_s)$ corrections when $\mu^2 = \mu_0^2 \gg \Lambda^2$. Having identified μ_0^2 as being a scale which leads to reasonable $\mathcal{O}(\alpha_s)$ corrections, we now ask: what happens when we vary μ^2 away from μ_0^2 ? Using (139) in the parton model expression, we see that there will be μ^2 dependent terms will be proportional to

$$\sigma(\mu^2) - \sigma(\mu_0^2) \sim \left[\frac{\alpha_s}{2\pi} \ln(\mu^2/\mu_0^2) \right]^2 \sim \left[\frac{\ln(\mu^2/\mu_0^2)}{\ln(\mu^2/\Lambda^2)} \right]^2 \quad (142)$$

times an overall factor having roughly the same magnitude as the Born term. For typical values of μ and α_s , $\frac{\alpha_s}{2\pi} \ln(\mu^2/\mu_0^2)$ is a small number so that the μ^2 dependence is rather suppressed so long as μ^2 is not too far from μ_0^2 . These terms will only cancel when two-loop corrections to the subprocess cross section are included. There are also terms with lower powers of $\ln(\mu^2/\mu_0^2)$ (i.e. from (137)) which require two-loop corrections for cancellation as well.

The next question is: how much better are we doing than a Born level calculation? In the Born level result, the μ^2 dependence comes entirely from the evolution of the distributions. Hence, from (134), (139),

$$\sigma_{\text{Born}}(\mu^2) - \sigma_{\text{Born}}(\mu_0^2) \sim \frac{\alpha_s}{2\pi} \ln(\mu^2/\mu_0^2), \quad (143)$$

again times an overall factor having roughly the same magnitude as the Born term. We see explicitly that inclusion of one-loop corrections reduces the μ^2 dependence by an extra factor of $\frac{\alpha_s}{2\pi} \ln(\mu^2/\mu_0^2)$ for reasonable values of μ^2 . The above arguments apply to all one loop calculations in hadronic processes. In general, though, there is also a contribution from the evolution of the gluon distribution at $\mathcal{O}(\alpha_s)$, relative to the Born term. This is because, in general, the gluon distribution may enter in the Born term. Then, imposing the analogue of (136) would determine $c_{1,k}^g$ as given by (141).

One could also convolute the Born cross sections with parton distributions having no evolution (i.e. determined at some fixed scale $\bar{\mu}^2$), which would correspond to an “off-shell” renormalization of the parton distributions in higher order. But then the physical predictions would be wrong by terms $\sim \frac{\alpha_s}{2\pi} \ln(\mu_0^2/\bar{\mu}^2)$, since the one loop corrections would contain such terms (analogous to the terms $\sim \frac{\alpha_s}{2\pi} \ln(M^2/\mu^2)$ present in (131), (132)). So, even though there is no renormalization scale dependence, the error will be larger for $\mu_0 \gg \bar{\mu}$ or $\mu_0 \ll \bar{\mu}$. One expects an analogous tradeoff when using one-loop evolution instead of two-loop evolution in NLO calculations.

Actually, this argumentation is somewhat naive in the sense that we only considered explicitly the $\sim [\frac{\alpha_s}{2\pi} \ln(\mu^2/\mu_0^2)]^2$ behavior. For processes such as the Drell-Yan process, which receive large π^2 corrections, there will be residual μ^2 -dependent effects arising from the μ^2 -dependent part of the parton distributions multiplied by the large correction terms in the cross section which will not cancel at the one-loop level. Thus, there will be an additional μ^2 dependence of the cross section proportional to

$$\sigma^{\pi^2}(\mu^2) - \sigma^{\pi^2}(\mu_0^2) \sim \frac{\alpha_s}{2\pi} \pi^2 \left[\frac{\alpha_s}{2\pi} \ln(\mu^2/\mu_0^2) \right] \quad (144)$$

$$\sim \frac{\pi}{2} \alpha_s \left[\frac{\alpha_s}{2\pi} \ln(\mu^2/\mu_0^2) \right], \quad (145)$$

which is still suppressed relative to the μ^2 dependence of the Born term for typical energy scales. Of course, there may be other sources of large corrections not strictly proportional to π^2 (see the discussion near the beginning of section XI), so our π^2 factor is really a generic representation of large correction terms in general. The rule then is that the larger the one-loop corrections, the greater the μ^2 dependence. Inclusion of two-loop corrections (and evolution) will reduce this factor. We will not discuss two-loop effects in any detail here. Also, we will not perform detailed numerical studies of scale dependence, as this has been done extensively in the literature. The above discussion was included simply to clarify the origin of the scale dependence and to show how it is reduced by the inclusion of QCD corrections in general.

IX. DRELL-YAN IN LOW ENERGY RUNNING AT RHIC

Throughout, for unpolarized cross sections, we use subprocess cross sections determined in the $\overline{\text{MS}}$ scheme of DREG. They are convoluted with the unpolarized MRSG set [41] of parton distributions. Varying the choice of unpolarized parton distributions produces negligibly small changes in the spin dependent asymmetries in general. Hence, we only consider the effect of varying the polarized parton distributions even though, strictly speaking, one should use specific unpolarized sets with the various polarized sets. We use the GSA and GSC sets [42] as well as the GRSV (standard NLO $\overline{\text{MS}}$) set [43] and compare the corresponding predicted asymmetries. Since all these sets are determined in the $\overline{\text{MS}}_{HC}$ scheme, using HVBm regularization, we use subprocess cross sections determined in that scheme for doubly polarized predictions. Clearly then, for single-spin cross sections, we use the $\overline{\text{MS}}_{HC}(\overline{\text{MS}})$ scheme for the renormalization of the (un)polarized parton distributions which enter (i.e. for the

T_{ij}). Consequently, the $\Delta_k P_{ij}^\varepsilon$ are always those of DREG/HVBM, given in Eq's (29) and (30). Throughout, we use a two-loop evolved α_s , with 5 flavors. We also use $\mu = M$ in all numerical calculations.

We will always present both the LO and NLO results for the asymmetries given. We use NLO parton distributions, polarized and unpolarized, in all asymmetries however. The reason, as discussed in section VII, is that the LO parton distributions possess a process dependence of order α_s , while the NLO ones are process dependent only at order α_s^2 . Therefore, it is in general not meaningful to use LO parton distributions in making predictions for processes with different structure from the one where they were determined; in the polarized case, DIS. In this way, our LO and NLO asymmetries are closer to the actual first two terms in the “all-orders” expansion of the asymmetry in α_s and the difference in the LO and NLO predictions meaningfully measures the effect of the HOC. Finally, if one uses the LO polarized distributions determined from DIS, one would also have to use LO unpolarized distributions determined entirely from DIS as well, for consistency.

In order to understand the qualitative features of the numerical results, in pp collisions, it is instructive to examine which values of x are being probed in the parton distributions for a given M . We will consider the leading order contributions for simplicity. From (18), we see that $d\sigma/dM$ involves an integration over $x_F (= x_{F0})$, equivalent to a single integration over x_a (or x_b), both constrained by (19) with $w = 1$. $d\sigma/dMdx_F$ can be obtained from (23), though, and involves no integration. Numerically, it is found to generally peak at $x_F \simeq 0$. This implies that dominant contributions come from the region $x_a \simeq x_b \simeq \sqrt{\tau}$. The peak is not very sharp though, so this is somewhat of an approximation. Nonetheless, this feature holds for the energies considered here and becomes more pronounced with decreasing τ . The basic reason is that at $x_a = x_b = \sqrt{\tau}$ there is an equal contribution coming from the $q\bar{q}$ and $\bar{q}q$ subprocesses. As one moves away from $x_F = 0$, one of the contributions becomes smaller since the \bar{q} distribution is being evaluated at larger x . This is somewhat compensated by the other term getting larger, especially at larger τ . Still, the net effect is a smaller contribution as x_F moves away from 0. As we go the lower τ , the fact that the peak is more pronounced is not so surprising due to the $1/(x_a + x_b)$ factor in $d\sigma/dMdx_F$, which is not present in the rapidity differential cross section. The rapidity differential cross sections generally peak at or near zero rapidity ($x_a = x_b$) as well, although the peak may be rather broad. x_F is more physical though, since it is simply $x_a - x_b$ at leading order (i.e. it is linear in x_a and x_b unlike the rapidity). Hence, in what follows, including after QCD corrections, we will assume that the qualitative features of the numerical results can be roughly described by taking $x_a \simeq x_b \simeq \sqrt{\tau}$. Of course, all figures are obtained using the exact expressions only, since the approximation does not give quantitatively accurate predictions. We will also use the shorthand notation,

$$q_{i,g} \equiv f_u^{q_{i,g}/p}(x, \mu^2), \quad \Delta q_i, \Delta g \equiv f_l^{q_{i,g}/p}(x, \mu^2), \quad (146)$$

with $x \simeq \sqrt{\tau}$. Also,

$$\sigma_{mn} \equiv d\sigma_{mn}^{pp,F+B}/dM, \quad (147)$$

where σ_{mn}^{F+B} was defined in (12) as being the usual leptonic integrated cross section.

Consider the double-spin asymmetry

$$A_{ll} \equiv \frac{1}{\mathcal{P}^A \mathcal{P}^B} \frac{\sigma_{ll}}{\sigma_{uu}}. \quad (148)$$

With the above mentioned assumptions, A_{ll} is roughly given by

$$A_{ll} \simeq - \frac{(4/9)\Delta u \Delta \bar{u} + (1/9)\Delta d \Delta \bar{d} + (1/9)\Delta s \Delta \bar{s}}{(4/9)u\bar{u} + (1/9)d\bar{d} + (1/9)s\bar{s}}. \quad (149)$$

Due to the extra factor of 4 and the relative largeness of the u_v and Δu_v distributions, the cross section and asymmetry are mostly dominated by the up quarks.

The polarized valence distributions are reasonably well constrained over a large range of x from polarized DIS. The polarized sea quark distributions, however, are only moderately constrained at smaller x , where their contribution in DIS is non-negligible. At moderate and large x , there is no constraint experimentally on the polarized sea quark distributions, as they are vanishingly small compared to the valence ones.

Most models, however, assume the behaviour

$$|\Delta q_v|/q_v \xrightarrow{x \rightarrow 1} 1, \quad |\Delta q_v|/q_v \xrightarrow{x \rightarrow 0} 0, \quad (150)$$

which appears to be consistent with the DIS data. The result is that the asymmetries, and the distinction between the various polarized sets, will be largest at large τ (i.e. large x) where the cross sections are small. Conversely, where the cross sections are large (small τ) we expect small asymmetries if the polarized sea quark distributions are small at low x , as all the sets assume.

Fig. 1(a) gives the (virtual photon dominated) unpolarized Drell-Yan cross section, $d\sigma/dM$, at $\sqrt{S} = 100$ GeV, versus M for pp collisions relevant to RHIC. Here, we include only one type of lepton pair (i.e. $\mu^+ \mu^-$). Throughout, we present the leading order, next-to-leading order with $q\bar{q}$ contributions only, and full next-to-leading order

predictions for all cross sections and asymmetries. This means that, for the asymmetries, the numerators and denominators are treated in the same way with regard to which corrections are included. Here and throughout, we note that the $q\bar{q}$ corrections are positive and large. The qg subprocess makes a small negative contribution though. This highlights the fact that one cannot think of the qg subprocess as being physically separate from the $q\bar{q}$ subprocess. They are both related via the renormalization of the quark distributions. We will now investigate this issue thoroughly.

The negativity of the qg contribution also holds in the $\overline{\text{MS}}_\epsilon$ scheme. This will (slightly) simplify the process of understanding the origin of the negative qg contribution. The analytical result for the subprocess cross section is given in (132). Since, when using $\overline{\text{MS}}_\epsilon$ factorization, the scheme dependent part of the subprocess cross section is zero and since $k_{mn}^{qg, F+B}(w) > 0$ and since $\mu^2 = M^2$ here, the only negative contribution comes from the term $\sim \Delta_u P_{qg}^4(w) \ln(1-w)$. From (78), (87), (88), (92) we see that this term arose from $(1-w)^{-2\epsilon} \Delta_u P_{qg}^4(w)/\epsilon$ and is therefore of collinear origin. This means that such terms could be factorized via the renormalization of the quark distributions, but would most likely lead to unphysical distributions violating some of the conservation rules mentioned in Sec. VII. So, we see explicitly that the issue of the negativity of the qg subprocess is intimately related to the issue of the renormalization of the quark distribution, which in turn connects the $q\bar{q}$ and qg subprocesses.

The fact that the net qg contribution is negative tells us something about which regions of the w integration are giving dominant contributions. In order that the qg contribution be negative, we see from (132) that we must satisfy

$$\Delta_u P_{qg}^4(w) [2 \ln(1-w) - \ln w] + \frac{(1-w)}{4} (1+3w) < 0 \quad (151)$$

(again working in the $\overline{\text{MS}}_\epsilon$ scheme for simplicity). This is satisfied for

$$w > .572022. \quad (152)$$

Since the w integration includes $w = 1$, we expect large contributions from the term $\sim \ln(1-w)$ from w near 1. In light of (152), we can see clearly why the corrections are negative.

The expected yearly integrated RHIC pp luminosity at $\sqrt{S} = 100$ GeV is $\mathcal{L} = 160 \text{ pb}^{-1}$ (assuming it is linear in \sqrt{S} down to this energy). This means that the statistics will be quite poor beyond $M = 20$ GeV, concerning asymmetry measurements, whose error goes like (see (20))

$$\Delta A_{mn} = \sqrt{\frac{1 - A_{mn}^2}{N}} \frac{1}{S_m^A S_n^B} \simeq \frac{1}{\sqrt{N}} \frac{1}{S_m^A S_n^B}, \quad A_{mn} \equiv \frac{\sigma_{mn}}{\sigma_{uu}} \frac{1}{S_m^A S_n^B}, \quad (153)$$

where the approximate equality holds for A_{mn} not too large. Here N is the number of events. Assuming 1 GeV binning, this means that for $M \simeq 5$ GeV, $\Delta A_{ll} \simeq .4\% / \mathcal{P}^A \mathcal{P}^B$. Unfortunately, this is a rather low mass scale where the parton model may not work well. For $M \simeq 10$ GeV, $\Delta A_{ll} \simeq 1.8\% / \mathcal{P}^A \mathcal{P}^B$. At low M ($\lesssim 10$ GeV), one also has to be careful of resonance backgrounds. Experimental cuts will make the errors slightly larger. On the other hand, with two independent experiments (at the PHENIX and STAR detectors), the combined asymmetry measurements should have roughly the errors given here. A more detailed error analysis is beyond the scope of this paper.

Fig. 1(b) gives the corresponding A_{ll} . The behaviour is exactly as expected from the previous arguments. In the low mass region, where the statistics are good, A_{ll} is of the order 1–2%. There is also little distinction between the various sets. This is a result of the common assumptions

$$|\Delta \bar{u}|/\bar{u} \ll 1, \quad \Delta \bar{u} < 0 \quad (\text{at small } x). \quad (154)$$

There is certainly more freedom in $\Delta \bar{q}$ than is manifest among the various sets. The DIS constraints on $\Delta \bar{q}$ are rather weak and it will be interesting and important to see whether or not the low mass Drell-Yan asymmetry is as small (and positive) as it is predicted to be.

It is also of interest to study the effect of the QCD corrections on A_{ll} . From Fig. 1(b), we observe good stability in the $q\bar{q}$ contribution in general. This is not unexpected, taking into account helicity conservation. For the GRSV and GSA sets, Δg is positive and sizable. For the GSC set, Δg is positive at small x , but negative and small at large x . Hence, the gluonic contribution is small and uninteresting in general for the GSC set. Therefore, we study throughout the gluonic contributions (and features in general) only for the GRSV and GSA sets. We notice that the gluonic contribution to A_{ll} is always positive. The gluonic contributions to σ_{ll} and σ_{uu} are dominated by the ug subprocess. Since both Δu and Δg are positive, the essential difference between the sign of the gluonic contribution to σ_{ll} and σ_{uu} is that arising from the sign of the respective subprocess cross sections. The most important difference between $\hat{\sigma}_{ll}^{qg}$ and $\hat{\sigma}_{uu}^{qg}$ is the difference in the overall factors (which are proportional to the respective Born terms, see (73)–(75)). There is a relative minus in the overall factors for $\hat{\sigma}_{uu}^{qg}$ and $\hat{\sigma}_{ll}^{qg}$.

More precisely, for the correction, $\hat{\sigma}_{ll}^{qg}$, to be positive, we must satisfy (151) with $\Delta_u P_{qg}^4(w)$ replaced by $\Delta_l P_{qg}^4(w)$. It is satisfied for

$$w < .208233, \quad w > .652396. \quad (155)$$

Using the same logic as before, dominant contributions will come from near $w = 1$, where the corrections are positive. Hence the corrections to σ_{ll} will be positive. The qg corrections to σ_{ll} are relatively larger than those to σ_{uu} since, for typical x and μ^2 ,

$$|\Delta g/\Delta \bar{q}| > g/\bar{q}, \quad (156)$$

in the sets considered. Hence the qg subprocess typically weighs in more heavily versus the $q\bar{q}$ subprocess in σ_{ll} than in σ_{uu} . Thus we can clearly understand the sizable and positive qg corrections to A_{ll} . This rationale also applies to the corrections to A_{ll} in Z - and W^\pm -boson production.

Figures 2(a) and 2(b) show the corresponding cross sections and asymmetries at $\sqrt{S} = 200$ GeV. All the features are the same. The luminosity is doubled and the unpolarized cross sections are larger for the same M (due to the smaller x , where the sea quark distributions are large). The asymmetries are somewhat smaller though. Hence the statistical significance ($\Delta A_{ll}/A_{ll}$) is comparable. The main difference is that we probe lower x than at $\sqrt{S} = 100$ GeV. Running at more than one energy is definitely an advantage in that one covers a larger range of x and μ^2 , compared with only running at one energy. This also allows some degree of cross checking via perturbative evolution and thus allows detection of various types of systematic errors. The net result is lower overall errors on the polarized parton distributions so determined.

X. Z-BOSON PRODUCTION AT RHIC

Z -boson production at RHIC is quite useful since it allows us to measure the polarized parton distributions at relatively large x . Also, the parton distributions enter as a different linear combination in the Z double-spin asymmetries than for production by virtual photons. This is helpful for disentangling the various contributions. One can also make use of parity violation to consider additional asymmetries which vanish for virtual photon production. The major limitation is the event rate. Certain asymmetries will be able to somewhat overcome this limitation, however.

Fig. 3(a) shows the unpolarized cross section, $d\sigma/dM$ for $5 \leq M \leq 125$ GeV at $\sqrt{S} = 500$ GeV. Again, we consider production of only one type of lepton pair (i.e. $\mu^+\mu^-$). The QCD corrections behave analogously to the virtual photon case. Using the expected yearly integrated luminosity of 800 pb^{-1} and integrating the cross section between $80 \leq M \leq 100$ GeV gives approximately 8,000 $\mu^+\mu^-$ pairs. Hence we can measure asymmetries with an uncertainty (see (20), (153))

$$\Delta A_{mn} \simeq \frac{1 - 1.5\%}{S_m^A S_n^B}, \quad (157)$$

depending on the experimental cuts. Higher energy running would increase the Z event rate, but somewhat lower the asymmetries, as will become clear.

The double-spin asymmetry in the Z -pole region goes roughly like,

$$A_{ll} \simeq - \frac{\sum_q (g_{aq}^2 + g_{vq}^2) \Delta q \Delta \bar{q}}{\sum_q (g_{aq}^2 + g_{vq}^2) q \bar{q}}, \quad (158)$$

evaluated near $x \simeq \sqrt{\tau} = .18$. Putting in the appropriate couplings gives

$$A_{ll} \simeq - \frac{.29 \Delta u \Delta \bar{u} + .37 (\Delta d \Delta \bar{d} + \Delta s \Delta \bar{s})}{.29 u \bar{u} + .37 (d \bar{d} + s \bar{s})}. \quad (159)$$

In general, for Z production, the GSA and GRSV sets correspond to two extreme solutions, with the GSC set lying somewhere in between. So, as in the last section, we will try to understand qualitatively only the GSA and GRSV predictions, since one can make a clear prediction for those sets.

All sets assume an $SU(3)$ symmetric polarized sea and take a negative down valence and a positive up valence distribution. For the GRSV set, the sea quark distributions are negative everywhere, while for the GSA set they are positive at intermediate and large x and become negative only at small x . Thus, for the GSA set, $\Delta \bar{q} > 0$ in the x range of interest, $x \simeq .18$.

There will be some cancellation between the up- and down-quark contributions, but since

$$\frac{\Delta u_v(.18)}{-\Delta d_v(.18)} \simeq 2.5 - 4, \quad (160)$$

the u contribution will still be bigger. Due to the smallness of the polarized sea quark distributions, $\Delta q \simeq \Delta q_v$. Hence, we expect

$$A_{ll} > 0 : \text{GRSV}, \quad A_{ll} < 0 : \text{GSA} \quad (161)$$

in the Z -pole region.

Fig. 3(b) presents A_{ll} for $5 \leq M \leq 125$ GeV. The higher order corrections (HOC) have the same behaviour as for virtual photon production, for exactly the same reasons. As well, the sign of A_{ll} predicted in (161) is verified. There is roughly a 4% variation in A_{ll} between the two extreme cases. This means that one can rule out one case or the other, but not much more. Hence we must examine other asymmetries in order to do better. It would also be interesting to look at A_{ll} in the low mass region, where the virtual photons dominate, due to the large event rate. As mentioned in the previous section, A_{ll} may turn out to be larger than expected in that region.

Define the single-spin asymmetry as

$$A_l \equiv A_{ul} = \frac{1}{\mathcal{P}^B} \frac{\sigma_{ul}}{\sigma_{uu}} = A_{lu} = \frac{1}{\mathcal{P}^A} \frac{\sigma_{lu}}{\sigma_{uu}}. \quad (162)$$

There is an overall minus relative to the definition often used [44], owing to (14), (15). This asymmetry is nonzero due to the parity violating Z vertices. It is approximately given by

$$\begin{aligned} A_l &\simeq \frac{\sum_q [2g_{aq}g_{vq}(q\Delta\bar{q} - \bar{q}\Delta q)]}{\sum_q [(g_{aq}^2 + g_{vq}^2)(2q\bar{q})]} \\ &= \frac{g_{au}g_{vu}u_v\Delta\bar{u} + g_{ad}g_{vd}d_v\Delta\bar{d}}{(g_{au}^2 + g_{vu}^2)u\bar{u} + (g_{ad}^2 + g_{vd}^2)(d\bar{d} + s\bar{s})} \\ &\quad - \frac{g_{au}g_{vu}\bar{u}\Delta u_v + g_{ad}g_{vd}\bar{d}\Delta d_v}{(g_{au}^2 + g_{vu}^2)u\bar{u} + (g_{ad}^2 + g_{vd}^2)(d\bar{d} + s\bar{s})} \\ &\simeq \frac{.1u_v\Delta\bar{u} + .17d_v\Delta\bar{d}}{.29u\bar{u} + .37(d\bar{d} + s\bar{s})} - \frac{.1\bar{u}\Delta u_v + .17\bar{d}\Delta d_v}{.29u\bar{u} + .37(d\bar{d} + s\bar{s})}, \end{aligned} \quad (163)$$

where we took $(\Delta)q(x) = (\Delta)\bar{q}(x)$ as is done in all the sets considered. Noting that

$$\frac{\bar{d}(.18)}{\bar{u}(.18)} \simeq 2 \quad (164)$$

and taking into account (160), we observe a rather large cancellation between the $\bar{u}\Delta u_v$ and $\bar{d}\Delta d_v$ contributions in the second term of (163). The net effect is that the first and second terms become comparable in magnitude. Hence A_l is directly sensitive to $\Delta\bar{u}$ and $\Delta\bar{d}$. Also, the $\Delta\bar{u}$ and $\Delta\bar{d}$ contributions are comparable, unlike in virtual photon production. The second term is reasonably well constrained from DIS, while the first term is almost completely unconstrained (except in maximum magnitude). From the respective signs of the sea quark distributions, we expect A_l to be most positive for the GSA set and least so for the GRSV set.

Fig. 4(a) shows A_l for $5 \leq M \leq 125$ GeV. We observe the predicted behaviour. At small M , A_l vanishes as expected since the parity violating Z contribution also vanishes. The peak is just above the Z -pole and there is a well measurable separation between the various sets. So, the sensitivity to the sea quark distributions has improved as compared to A_{ll} .

One can take advantage of having two polarized beams to improve the statistical significance of the parity violating asymmetry. Define the two-spin parity violating asymmetry as,

$$A_{ll}^{PV} \equiv \frac{\sigma(+,+) - \sigma(-,-)}{\sigma(+,+) + \sigma(-,-)} \Big|_{\mathcal{P}^A, \mathcal{P}^B=1} = \frac{2(\sigma_{ul}/\mathcal{P}^B + \sigma_{lu}/\mathcal{P}^A)}{2(\sigma_{uu} + \sigma_{ll}/\mathcal{P}^A\mathcal{P}^B)} \quad (165)$$

$$\simeq \frac{2}{\mathcal{P}} \frac{\sigma_{ul}}{\sigma_{uu}}, \quad \text{for } \mathcal{P}^A \simeq \mathcal{P}^B \equiv \mathcal{P}, \quad (166)$$

where the last approximate equality holds since $\sigma_{ll} \ll \sigma_{uu}$ as σ_{ll} involves two polarized parton distributions and is thus relatively rather suppressed. We see explicitly that A_{ll}^{PV} is proportional to $1/\mathcal{P}$ (relative to experiment), not $1/\mathcal{P}^2$ as is often assumed. In order to get an idea of the statistical error on A_{ll}^{PV} , we will make the simplifying assumption that, experimentally, $\mathcal{P}^A = \mathcal{P}^B = 1$. Then, the total number of events is given by

$$\begin{aligned} N_0 &= \mathcal{L} \frac{\sigma(+,+) + \sigma(-,-)}{4} = \mathcal{L} \frac{\sigma_{uu} + \sigma_{ll}}{2} \\ &\simeq \mathcal{L} \frac{\sigma_{uu}}{2}, \end{aligned} \quad (167)$$

assuming equal running in all four polarization modes. Hence, the number of events is cut in half, but the asymmetry is doubled. So,

$$\frac{\Delta A_{ll}^{PV}}{A_{ll}^{PV}} \simeq \frac{1}{\sqrt{2}} \frac{\Delta A_l}{A_l}. \quad (168)$$

This means that we gain roughly a factor of $\sqrt{2}$ in precision by looking at A_{ll}^{PV} . One could argue, of course, that there are two A_l ; A_{ul} and A_{lu} . Then, one could combine them to improve the errors. Theoretically, the

two asymmetries are equal, but experimentally they only approach each other in the limit of infinite events. The problem is that these are not independent measurements. Hence, one cannot simply add the ΔA_l in quadrature. If we define \bar{A}_l as being the experimental average of the two A_l , a proper treatment of the errors yields

$$\begin{aligned}\frac{\Delta \bar{A}_l}{\bar{A}_l} &= \frac{1}{\sqrt{N_0}} \left[\frac{1 - A_l^{PV2}}{A_l^{PV2}} + \frac{A_l^{PV} - \bar{A}_l}{A_l^{PV}} \right]^{1/2} \\ &\simeq \frac{1}{\sqrt{N_0}} \left[\frac{1 - A_l^{PV2}}{A_l^{PV2}} + \frac{1}{2} \right]^{1/2}.\end{aligned}\quad (169)$$

In the limit of small A_l^{PV} , $\Delta \bar{A}_l / \bar{A}_l \rightarrow \Delta A_l^{PV} / A_l^{PV}$, but in general $\Delta \bar{A}_l / \bar{A}_l > \Delta A_l^{PV} / A_l^{PV}$. Statistically, one therefore does best with A_l^{PV} when two polarized beams are available. Although, \bar{A}_l is not much worse for typical experiments, Z production in particular, where the fractional errors should be virtually identical in \bar{A}_l and in A_l^{PV} . Of course, the above analysis is only strictly valid in the limit of full beam polarization. Inclusion of partial beam polarization will not change our conclusions, however, since we can always ‘pretend’ that the beams are fully polarized. Then we are measuring the polarized parton distributions multiplied by the corresponding beam polarizations, rather than just the distributions themselves. When considering x_F (or rapidity) differential cross sections, A_l is the quantity of interest [44] since it is more directly related to the ratio of the polarized to unpolarized parton distributions.

Fig. 4(b) gives A_l^{PV} for $5 \leq M \leq 125$ GeV. It has exactly the expected behaviour. Since $\Delta A_l^{PV} \simeq (1.5 \sim 2\%) / \mathcal{P}$, we can clearly distinguish between the possible solutions, and hence are quite sensitive to both $\Delta \bar{u}$ and $\Delta \bar{d}$ in the region $x \simeq .18$.

XI. W^\pm -BOSON PRODUCTION AT RHIC

It is important to determine the intermediate- and large- x behaviour of the antiquark distributions at high μ^2 since this (along with the large- x gluonic behaviour) influences the behaviour of the antiquark distributions in the limit $x \rightarrow 1$ at lower μ^2 , relevant to deep-inelastic scattering. This is because when one evolves from a low energy scale to a high energy scale, the large- x behaviour influences the evolution at lower x , and vice-versa. Using W^\pm production at RHIC, we can gain insight into the $x \rightarrow 1$ behaviour of the antiquark distributions, where other experiments (such as deep-inelastic scattering) will have little or no sensitivity. This statement applies equally to the polarized and unpolarized antiquark distributions in the proton.

W^\pm production at RHIC is ideally suited for this purpose because of the high event rate, resulting from RHIC’s high luminosity, and because of the flavor specificity of the cross sections. In Figures 5(a) and 5(b), respectively, we plot the $W^+ \rightarrow l^+ \nu_l$ and $W^- \rightarrow l^- \bar{\nu}_l$ production cross sections for $200 \leq \sqrt{S} \leq 700$ GeV and for decay into one type of lepton (i.e. muons). Since one cannot measure M on an event by event basis, we have integrated over it. The HOC have the same structure as for γ^* and Z production. At this point though, it is instructive to look at the variation of the QCD corrections with \sqrt{S} . We understand the origin of the negative $q\bar{q}$ contribution, from the discussion in section IX. The fact that the relative magnitude of the $q\bar{q}$ contribution increases with \sqrt{S} is understood to be a consequence of the increasing phase space in the initial state, reflected in a larger integration region over x_a and x_b (or w). What we are really observing is the effect of varying τ , since $M \simeq M_W$ for all \sqrt{S} .

One normally thinks of the large QCD corrections as arising mostly from the term $\sim \pi^2$ in the $q\bar{q}$ subprocess, which comes from the virtual corrections. The rationale is that all the other terms are of order one and will tend to largely cancel among themselves. Clearly, things are somewhat more subtle than that though, since the term ~ -7 in (71) makes the finite virtual corrections small and negative. Also, the corrections to the $q\bar{q}$ subprocess clearly increase with decreasing \sqrt{S} (i.e. increasing τ). In order for the net correction to be positive, there must be a large, positive contribution arising from the $q\bar{q}$ bremsstrahlung. Such a large term is indeed present in (131), namely, the term $\sim -4(1+w)\ln(1-w)$ which gives a large, positive contribution from the integration region near $w = 1$. There is also a smaller term $\sim 4\ln^2(1-w_1)\delta(1-w)$ arising from the ‘+’-distribution term. As τ increases, these terms make a larger contribution relative to the other, potentially negative, bremsstrahlung contributions. The other term arising from the ‘+’-distribution could give rise to sizable positive corrections as well, but its exact relative magnitude depends on the details of the parton distributions. In the above picture, the behaviour of the corrections is well understood.

Considering the decay channel

$$W^\pm \rightarrow \mu^\pm \nu_\mu^{(-)}, \quad (170)$$

for $\sqrt{S} = 500$ GeV, one predicts roughly 105,000 $W^+(\mu^+)$ and 27,000 $W^-(\mu^-)$ events. Not taking into account the details of the cuts, this corresponds roughly to an error on (double- and single-spin) asymmetries of

$$\Delta A_{mn}^{W^+} \simeq \frac{.3\%}{S_m^A S_n^B}, \quad \Delta A_{mn}^{W^-} \simeq \frac{.6\%}{S_m^A S_n^B}. \quad (171)$$

With such large rates at $\sqrt{S} = 500$ GeV, it is not unreasonable to consider going to lower \sqrt{S} as a way of probing larger x . In fact, the whole energy region,

$$250 \leq \sqrt{S} \leq 700 \text{ GeV}, \quad (172)$$

is interesting. Experimentally, the higher energies may be difficult to access. For the case of greatest experimental relevance (500 GeV), we are most sensitive to $x \simeq .16$.

The double-spin asymmetries adopt a simple form

$$A_{ll}^{W^+} \simeq -\frac{\Delta u \Delta \bar{d}}{ud}, \quad A_{ll}^{W^-} \simeq -\frac{\Delta \bar{u} \Delta d}{\bar{u}d}, \quad (173)$$

so that $A_{ll}^{W^+}$ is sensitive to $\Delta \bar{d}$ and $A_{ll}^{W^-}$ is sensitive to $\Delta \bar{u}$. From the signs of the polarized antiquark distributions for the respective sets, we expect

$$\begin{aligned} \text{GSA} : A_{ll}^{W^+} &< 0, & A_{ll}^{W^-} &> 0, \\ \text{GRSV} : A_{ll}^{W^+} &> 0, & A_{ll}^{W^-} &< 0. \end{aligned} \quad (174)$$

$A_{ll}^{W^+}$ and $A_{ll}^{W^-}$ are shown in Figures 6(a) and 6(b), respectively. The signs are as expected. We also see that $|A_{ll}|$ increases as \sqrt{S} decreases (i.e. x increases), which is a consequence of (150). This is a general trend which makes low energy measurements feasible. With high precision A_{ll} measurements possible at $\sqrt{S} = 500$ GeV, there is no problem in disentangling $\Delta \bar{u}$ and $\Delta \bar{d}$ near $x = .16$.

For $A_{ll}^{W^+}$, the HOC's have the same structure as $A_{ll}^{\gamma^*, Z}$, for the same reasons. For $A_{ll}^{W^-}$, the qg corrections have opposite sign since it is now the dg subprocess which enters. Another interesting feature of this and other asymmetries in W^\pm production is that the effect of the HOC is comparable to the expected uncertainty in their measurement. Hence, a complete analysis must make use of the QCD corrections in order not to waste the good statistics.

The W^+ single-spin asymmetry is roughly

$$A_l^{W^+} \simeq \frac{u \Delta \bar{d}}{2ud} - \frac{\bar{d} \Delta u}{2u\bar{d}} = \frac{\Delta \bar{d}}{2\bar{d}} - \frac{\Delta u}{2u} < 0. \quad (175)$$

The second term is dominant over the first, but the first term does allow distinction between sets. We expect, based on the signs of the various $\Delta \bar{d}$,

$$|A_l^{W^+}(\text{GRSV})| > |A_l^{W^+}(\text{GSA})|. \quad (176)$$

The W^- single spin asymmetry is approximately

$$A_l^{W^-} \simeq \frac{d \Delta \bar{u}}{2d\bar{u}} - \frac{\bar{u} \Delta d}{2\bar{u}d} = \frac{\Delta \bar{u}}{2\bar{u}} - \frac{\Delta d}{2d} > 0. \quad (177)$$

Now the two terms are more comparable in magnitude, since $\bar{u} < \bar{d}$ at large x and all the sets assume $\Delta \bar{u} = \Delta \bar{d}$. Thus, the magnitudes of $\Delta \bar{u}$ and Δd are important as is the sign of $\Delta \bar{u}$. In this case, we expect

$$A_l^{W^-}(\text{GSA}) > A_l^{W^-}(\text{GRSV}), \quad (178)$$

since there is a cancellation in the GRSV case. In the GSA case, there is an enhancement rather than a cancellation and we expect large asymmetries at small \sqrt{S} , where x is large.

Figures 7(a) and 7(b) present $A_l^{W^+}$ and $A_l^{W^-}$, respectively. We see that the behaviour is exactly as expected. In all cases, distinction between the various sets is straightforward; more so for $A_l^{W^-}$, however. For $A_l^{W^+}$, knowledge of the HOC's are particularly important for this separation, especially at lower \sqrt{S} . For $A_l^{W^-}$, we probe $\Delta \bar{u}$ in a very direct fashion. The asymmetries are large throughout. They are roughly constant for the GRSV set, but increase in magnitude in the GS case as we go to lower energies, allowing a precise determination of $\Delta \bar{u}$ over a wide range of x . Of course, no single measurement should be expected to determine any specific parton distribution exactly. One must fit all the data, including the DIS data.

Figures 8(a) and 8(b) give A_{ll}^{PV} for W^+ and W^- production, respectively. We notice again roughly a factor of 2 enhancement over A_l , except near $A_{ll}^{PV} = 1$, where we are of course constrained by $A_{ll}^{PV} \leq 1$. Already, precision A_l measurements were possible, so A_{ll}^{PV} , with the extra $\sqrt{2}$ in precision, can pin down rather tightly the allowed sets of parton distributions.

Z and W^\pm production at RHIC have been previously examined in LO as a tool for pinning down the polarized parton distributions in [44,45]. In those studies (Z and W^\pm) rapidity differential asymmetries were considered, which are quite useful in pinning down the x -dependence of the parton distributions. The general conclusions are the same. Also, transverse momentum distributions for Z and W^\pm production at RHIC were studied using Monte

Carlo methods which sum up certain bremsstrahlung graphs in [46]. This observable is known to be sensitive to the polarized gluon distribution.

Another interesting issue is the ratio \bar{u}/\bar{d} at large x and μ^2 , which is unrelated to spin physics. Knowledge of the \bar{u}/\bar{d} ratio at large x and μ^2 gives information on that ratio at even larger x at lower μ^2 , where there is very little experimental information. This was discussed at the beginning of this section. DIS is insensitive to the sea quarks at large x , since they are masked by the valence quark distributions.

From the experimentally measured violation [47] of the Gottfried sum rule [48], we can conclude that $\bar{u}(x) \neq \bar{d}(x)$ for all x . Maximal violation of SU(2) flavor symmetry is usually taken to occur at larger x , where RHIC is sensitive. A typical assumption for x (and μ^2) accessible to RHIC in W^\pm production is $\bar{u}/\bar{d} \simeq .5$ [41]. This is based on the Pauli exclusion principle and explaining the Gottfried sum rule violation. The idea is that since the relative number of valence to sea quarks is increasing with x , the Pauli suppression effect will increase with x such that the \bar{u}/\bar{d} ratio decreases as there are more up valence quarks than down valence quarks, leading to greater suppression of the up sea. More recently, low energy fixed target Drell-Yan experiments at Fermilab have helped to disentangle \bar{d} and \bar{u} at lower μ^2 .

The quantity of experimental interest (again considering the muonic decay channel) is

$$R_W \equiv \frac{\sigma(W^-)}{\sigma(W^+)} \simeq \frac{d\bar{u}}{d\bar{d}}, \quad (179)$$

in crude approximation. Since the d and u contributions are quite well known, we directly probe \bar{u}/\bar{d} . With $\simeq 130,000$ events, we can measure R_W to high accuracy. At this level, we are again sensitive to the effect of the HOC's.

Fig. 9 shows R_W for $200 \leq \sqrt{S} \leq 700$ GeV. Two sets are considered. First, the MRSG set and second, the MRSG set with \bar{d} set equal to \bar{u} . We see a clear separation between the two possibilities for all \sqrt{S} . This will therefore be a crucial experiment for understanding the \bar{u}/\bar{d} ratio. This probe, at RHIC, has previously been studied in leading order and the same conclusions were drawn (see, for instance, [44,49]).

XII. THE FORWARD-BACKWARD DRELL-YAN ASYMMETRY

As discussed in the introduction, the principal purpose of performing a high precision measurement of the forward-backward Drell-Yan asymmetry at Fermilab is to precisely determine $\sin^2 \theta_W$. In order to accomplish this, it is necessary to take into account the QCD corrections. We have seen that in the case of the spin dependent asymmetries in pp collisions, the qg subprocess often destabilizes the asymmetry. As we will see, for the forward-backward asymmetry, the corrections arise predominantly from the $q\bar{q}$ subprocess. The explanation for this feature will be given in detail.

In Fig. 10(a), we present $d\sigma/dM$ for l^+l^- production in $p\bar{p}$ collisions at $\sqrt{S} = 1.8$ TeV. As usual, we include only one type of lepton-pair (i.e. $\mu^+\mu^-$ or e^+e^-). Also, as in the previous numerical calculations, we use the MRSG [41] unpolarized parton distributions in calculating physical cross sections. The peak in the cross section is quite a bit larger than at RHIC due to the higher energy (i.e. smaller x) and the valence-valence contributions. Here, and throughout, we use $\mu = M$. The effect of varying μ will be discussed later in this section.

Let us define the forward-backward (lepton) asymmetry as

$$A_{FB} = \frac{d\sigma_{uu}^{p\bar{p},F-B}/dM}{d\sigma_{uu}^{p\bar{p},F+B}/dM}, \quad (180)$$

where $\sigma^{F\pm B}$ were defined in (12). We expect large A_{FB} in $p\bar{p}$ collisions in mass regions where $Z - \gamma$ interference dominates since the asymmetry arises, at the subprocess level, from axial - vector interference so that the Z contribution is pure axial and the asymmetry is unsuppressed. At the Z -pole, on the other hand, the Z vector couplings enter and lead to a suppression, so the asymmetry will be somewhat smaller there. We can see this explicitly by noting that the leading order subprocess level asymmetry is proportional to

$$A_{FB}^{q\bar{q}} \sim \frac{g_{al}g_{aq}g_{vl}g_{vq}}{(g_{al}^2 + g_{vl}^2)(g_{aq}^2 + g_{vq}^2)} \quad (181)$$

at the Z -pole. Hence there is an overall small factor,

$$g_{vl} = -\frac{1}{2}(1 - 4\sin^2 \theta_W), \quad (182)$$

which is sensitive to $\sin^2 \theta_W$ since $\sin^2 \theta_W \simeq .23$, so that a small fractional change in $\sin^2 \theta_W$ leads to a large fractional change in A_{FB} .

Fig. 10(b) shows the effect of the QCD corrections on A_{FB} . We see that, unlike the spin asymmetries (double-spin in particular), it is the $q\bar{q}$ subprocess which accounts for the dominant corrections. We understand this in the following way. From Fig. 10(a), we see that the magnitude of the qg correction to σ^{F+B} is rather small compared

to that of the $q\bar{q}$ subprocess. Thus, in order for the qg subprocess to make an appreciable contribution to A_{FB} , the corrections to σ^{F-B} would have to be quite different from those to σ^{F+B} . Since one has the same parton distributions in both cases, all the difference arises from the differences in the subprocess cross sections. As we have explained before, the dominant corrections come from the term $\sim \ln(1-w)$ in (132) which has the same form in both σ^{F+B} and σ^{F-B} . Consequently, the qg corrections to $\sigma^{F\pm B}$ amount to a multiplicative factor which basically cancels in the ratio, in the mass region of interest. We also expect small corrections to A_{FB} arising from the $q\bar{q}$ subprocess, for the same reasons. The question then is: why are the $q\bar{q}$ corrections to A_{FB} observable while the qg corrections are not? The correction basically arises from the differences in the hard bremsstrahlung contributions to $\sigma^{F\pm B}$, $k_{uu}^{q\bar{q},F\pm B}$, given in (90). We note that the difference vanishes in the limit $w \rightarrow 1$, relevant for the large M limit and for the dominant corrections to $\sigma^{F\pm B}$ at lower M . This explains the vanishing of the corrections as M increases. At intermediate and low M , however, there will be some contribution to A_{FB} arising from smaller w , in which case the term, $k_{uu}^{q\bar{q},F-B} = 2(1+w)\ln w$, contributes negatively (oppositely to the Born term) in a significant fashion, thus accounting for the reduction in the magnitude of A_{FB} . Now, for the qg subprocess, the differences in the $k_{uu}^{qg,F\pm B}$ all vanish in the limit $w \rightarrow 1$ and are small at smaller w , thereby accounting for the relative smallness of the qg corrections to A_{FB} .

In the end, the corrections to A_{FB} almost exactly amount to a multiplicative factor (less than 1) which is given in Fig. 11. We see that it increases with increasing mass, approaching unity. In the Z -pole region, it is $\sim .975$. This result is in good agreement with the finding of [10], considering that they use a different definition of A_{FB} beyond LO, and a more involved approach, taking into account experimental cuts. Also, in their approach, one could not understand properly the structure of the QCD corrections, since the hard bremsstrahlung is handled via Monte Carlo integration. The spikes at $M \simeq 89.3 - 89.5$ GeV simply reflect the fact that A_{FB}^{NLO} and A_{FB}^{LO} vanish at *slightly* different points and intersect just above the zero.

Figures 12(a) and 12(b) show A_{FB} in the Z -pole region for $\sin^2 \theta_W = .2315$. The effect of the QCD corrections is shown as is the effect of changing $\sin^2 \theta_W$ by an amount of $\pm .0005$. The magnitudes of the effects are comparable, but the character is distinctly different. Changing $\sin^2 \theta_W$ amounts to a shift in A_{FB} rather than a multiplicative factor. As a result, changing $\sin^2 \theta_W$ shifts somewhat the zero of A_{FB} . Since the QCD corrections do not shift the zero appreciably, one sees that measuring precisely the zero in A_{FB} may allow one to get a good handle on $\sin^2 \theta_W$ without worrying about neglected higher order QCD effects (and possibly other uncertainties such as choice of parton distributions). How precisely this may be measured is left for a separate study. Using the GRV NLO ($\overline{\text{MS}}$) set [50] produced no appreciable change in the predictions. The CTEQ3M set [51], on the other hand, gave slightly different predictions for the forward-backward asymmetry. Hence, closer agreement between the various sets is required before precision determinations of $\sin^2 \theta_W$ are possible.

The fact that the zero of A_{FB} does not change appreciably under HOC's is understandable since the zero essentially arises from the zero in the subprocess cross section, which in turn depends on M in a way independent of parton distribution effects. Each subprocess, at NLO, is proportional to a Born term with a well-defined zero. So any shift in the zero must arise predominantly from the fact that each quark flavor passes through zero at slightly different values of M . The NLO corrections however, do not appreciably affect the weighting of the various quark flavors relative to the LO weightings, since the same parton distributions enter. Hence there is very little shift in the position of the zero.

We studied the effect of varying μ on A_{FB} and it was found to be negligible. This is not unexpected since the μ -dependent part of the corrections has the same form in σ^{F-B} and σ^{F+B} . Hence, the major uncertainties are in the parton distributions, the neglected nonleading corrections, the QED corrections and possible intrinsic transverse momentum effects. Normally, one would not consider the latter effects at such high μ^2 , but as we are dealing with a very high precision measurement, they should not be taken for granted as being negligible. There is also a pure QED contribution to A_{FB} at order α^3 , which was originally studied in connection with $e^+e^- \rightarrow \mu^+\mu^-$ [52].

With $\mathcal{L} = 110 \text{ pb}^{-1}$, A_{FB} for e^+e^- pairs in the Z -pole region was measured with a statistical error of roughly $\pm 20\%$ [53]. The maximum possible \mathcal{L} for Run II after several years running is 100 fb^{-1} [7]. We will take $\mathcal{L}_{\text{max}} = 70 \text{ fb}^{-1}$ as being a more realistic (if not optimistic) value in determining the best possible measurement of A_{FB} . Then, statistically, we expect to be able to measure A_{FB} to (at best) $\pm 8\%$. Hence, our statistical error goes down by a factor of roughly 25. The same statement applies to $\sin^2 \theta_W$. The statistical error on $\sin^2 \theta_W$ of $\pm .003$ which is obtained from 110 pb^{-1} is reduced to $\pm .00012$ with 70 fb^{-1} . If one takes into account two detectors and both muons and electrons, in a best case scenario, we could multiply our number of events by a factor of 4 and get $\pm .00006$ as an error on $\sin^2 \theta_W$. For a more realistic 30 fb^{-1} , we get an error of $\pm .00009 \simeq \pm .0001$. If we do not combine the data from both detectors, muons and electrons, this goes up to $\pm .0002$. Either way, the error is very small.

Of course, this error analysis is very naive and all the systematic errors must be put under tight control for a realistic ultrahigh precision measurement as discussed above. A more detailed analysis is beyond the scope of this paper. Nonetheless, if any of the above scenarios could be realized, this would be the best $\sin^2 \theta_W$ determination available. In fact, it would be better than the world average. Even with lower luminosity running such as 10 fb^{-1} and not combining muons and electrons, the measurement is of the same precision as the SLAC measurement and hence could help to resolve the SLAC-LEP discrepancy.

XIII. CONCLUSIONS

Complete analytical results for mass differential Drell-Yan type cross-sections relevant to all possible initial longitudinal polarization states were calculated at the one-loop level in QCD. Interference between bosons of arbitrary mass, width and couplings was considered. For all observables considered, the corresponding forward-backward cross sections were determined. The results were presented in a form valid for all consistent n -dimensional regularization schemes. A survey of constraints on allowable factorization and regularization schemes was given. The mechanism behind scale dependences was discussed in some detail and in a general fashion.

NLO predictions for all longitudinal Drell-Yan type processes at RHIC (W^\pm , Z and γ^*) were made using polarized parton distributions which fit the recent DIS data. The HOC's increased the cross sections substantially and had a major impact on the asymmetries, while preserving the features of the LO asymmetries. The exact sign and magnitude of the HOC's depended on the details of the polarized parton distributions used, especially the sea and gluon distributions. Faced with either low rates or small asymmetries, γ^* production did not appear very interesting at face value, for longitudinal polarization. On the other hand, if the agreement between the various parton distributions at small x is accidental, rather than constrained, γ^* production at RHIC could demonstrate that possibility by yielding an unpredicted asymmetry. The Z -asymmetries were all quite sensitive to the sea quarks; the parity violating ones being the largest, with unexpected sensitivity due to a coincidental cancellation between u and d valence contributions. With large rates and asymmetries, W^\pm production can directly measure the polarized sea and valence distributions as well as the unpolarized \bar{u}/\bar{d} ratio. Lower energy running could directly measure \bar{u} and \bar{d} at rather large x (both polarized and unpolarized).

NLO QCD predictions for the forward-backward lepton asymmetry at Fermilab were made. The QCD corrections amounted almost exactly to a multiplicative factor on the asymmetry which was a function of the mass of the lepton pair produced. This function was found to be less than unity throughout and approached 1 with increasing invariant mass. In the Z -pole region, the factor was roughly .975. It was thus observed that the zero in the asymmetry was quite stable under QCD corrections. The zero was rather sensitive to $\sin^2 \theta_W$, however. This suggested an alternate method for determining $\sin^2 \theta_W$ (i.e. measuring precisely the zero). The details were left for a separate study, however. Based on expected luminosities for Fermilab's Run II and previous Fermilab determinations which used a standard algorithm for extracting $\sin^2 \theta_W$ from A_{FB} , high precision $\sin^2 \theta_W$ measurements were found to be possible at a level much better than (statistically), or at worst competitive with, the best measurements presently available and should be able to resolve the SLAC-LEP discrepancy.

ACKNOWLEDGEMENTS

The author would like to thank W.J. Marciano for suggesting much of the work done here and for countless valuable discussions, without which, this project would not have been possible. I would also like to thank F.E. Paige for insightful discussions and suggestions, which stimulated my interest in some of the work done. I also acknowledge very useful discussions with G. Bunce, P. van Nieuwenhuizen, N. Saito, M. Tannenbaum and T.L. Trueman as well as useful correspondence with W. Vogelsang. Finally, I would like to thank Z. Parsa and the ITP of UCSB, where part of this work was done, for their hospitality during the workshop on future high energy colliders. Supported by U.S. Department of Energy contract number DE-AC02-76CH00016.

-
- [1] P. Ratcliffe, Nucl. Phys. **B223**, 45 (1983).
 - [2] A. Weber, Nucl. Phys. **B382**, 63 (1992).
 - [3] A. Weber, Nucl. Phys. **B403**, 545 (1993).
 - [4] B. Kamal, Phys. Rev. D **53**, 1142 (1996).
 - [5] T. Gehrmann, Nucl. Phys. **B498**, 245 (1997).
 - [6] I. Alekseev et al., Preliminary Design Report, Polarized Proton Collider at RHIC, Jan. 1997.
 - [7] TeV-2000 Study Group, Report on Future Electroweak Physics at the Fermilab Tevatron, FERMILAB-PUB-96/082.
 - [8] G. Degrossi, P. Gambino and A. Sirlin, Phys. Lett. **394B**, 188 (1997).
 - [9] D.J.E. Callaway, Ann. Phys. **144**, 282 (1982); Phys. Lett. **108B**, 421 (1982).
 - [10] U. Baur, S. Keller and W.K. Sakumoto, Phys. Rev. D **57**, 199 (1998).
 - [11] C. Balázs and C.-P. Yuan, Phys. Rev. D **56**, 5558 (1997).
 - [12] G. 't Hooft and M. Veltman, Nucl. Phys. **B44**, 189 (1972).
 - [13] C.G. Bollini and J.J. Giambiagi, Nuovo Cim. B **12**, 20 (1972); Phys. Lett. **40B**, 566 (1972).
 - [14] W. Siegel, Phys. Lett. **84B**, 193 (1979).
 - [15] P. Breitenlohner and D. Maison, Commun. Math. Phys. **52**, 11 (1977).
 - [16] M. Chanowitz, M. Furman and I. Hinchliffe, Nucl. Phys. **B159**, 225 (1979).

- [17] A.P. Contogouris, S. Papadopoulos and F.V. Tkachov, Phys. Rev. D **46**, 2846 (1992); *Proceedings of the Joint International Lepton-Photon Symposium and Europhysics Conference on High Energy Physics*, Geneva, Switzerland, 1991, edited by S. Hegarty, K. Potter, and E. Quercigh (World Scientific, Singapore, 1992), Vol. 1, p. 450.
- [18] S. Kumano and M. Miyama, Phys. Rev. D **56**, 2504 (1997).
- [19] W. Vogelsang, Phys. Rev. D **57**, 1886 (1998).
- [20] A. Hayashigaki, Y. Kanazawa and Y. Koike, Phys. Rev. D **56**, 7350 (1997).
- [21] J.G. Körner, D. Kreimer and K. Schilcher, Z. Phys. C **54**, 503 (1992).
- [22] W. Siegel, Phys. Lett. **94B**, 37 (1980); L.V. Avdeev and A.A. Vladimirov, Nucl. Phys. **B219**, 262 (1983).
- [23] G. Altarelli and G. Parisi, Nucl. Phys. **B126**, 298 (1977).
- [24] R.K. Ellis, D. Ross and A. Terrano, Nucl. Phys. **B178**, 421 (1981).
- [25] L.E. Gordon and W. Vogelsang, Phys. Rev. D **48**, 3136 (1993).
- [26] A. Fiandrino and P. Taxil, Phys. Rev. D **44**, 3490 (1991).
- [27] W.J. Marciano and A. Sirlin, Nucl. Phys. **B88**, 86 (1975).
- [28] J.C. Ward, Phys. Rev. **78**, 182 (1950).
- [29] J.G. Körner, N. Nasrallah and K. Schilcher, Phys. Rev. D **41**, 888 (1990).
- [30] R.K. Ellis, M.A. Furman, H.E. Haber and I. Hinchliffe, Nucl. Phys. **B173**, 397 (1980).
- [31] R. Mertig and W.L. van Neerven, Z. Phys. C **70**, 637 (1996).
- [32] W. Vogelsang, Phys. Rev. D **54**, 2023 (1996); Nucl. Phys. **B475**, 47 (1996).
- [33] M. Stratmann and W. Vogelsang, Nucl. Phys. **B496**, 41 (1997).
- [34] I. Antoniadis and E.G. Floratos, Nucl. Phys. **B191**, 217 (1981).
- [35] Z. Kunszt, A. Signer and Z. Trócsányi, Nucl. Phys. **B411**, 397 (1994).
- [36] V.N. Gribov and L.N. Lipatov, Yad. Fiz. **15**, 781 (1972) [Sov. J. of Nucl. Phys. **15**, 438 (1972)]; Yad. Fiz. **15**, 1218 (1972) [Sov. J. of Nucl. Phys. **15**, 675 (1972)]; L.N. Lipatov, Yad. Fiz. **20**, 181 (1975) [Sov. J. of Nucl. Phys. **20**, 94 (1975)]; Yu. L. Dokshitzer, ZhETF **73**, 1216 (1977) [JETP **46**, 641 (1977)].
- [37] M. Stratmann, W. Vogelsang and A. Weber, Phys. Rev. D **53**, 138 (1996).
- [38] W. Vogelsang, Z. Phys. C **50**, 275 (1991).
- [39] G. Altarelli, R.K. Ellis and G. Martinelli, Nucl. Phys. **B157**, 461 (1979).
- [40] R. Hamberg, W.L. van Neerven and T. Matsuura, Nucl. Phys. **B359**, 343 (1991) and references therein.
- [41] A.D. Martin, R.G. Roberts and W.J. Stirling, Phys. Lett. **354B**, 155 (1995).
- [42] T. Gehrmann and W.J. Stirling, Phys. Rev. D **53**, 6100 (1996).
- [43] M. Glück, E. Reya, M. Stratmann and W. Vogelsang, Phys. Rev. D **53**, 4775 (1996).
- [44] C. Bourrely and J. Soffer, Phys. Lett. **314B**, 132 (1993).
- [45] J. Soffer and J.M. Virey, Nucl. Phys. **B509**, 297 (1998).
- [46] A. Saalfeld and A. Schäfer, Phys. Rev. D **57**, 3017 (1998).
- [47] P. Amaudruz et al. (New Muon Collaboration), Phys. Rev. Lett. **66**, 2712 (1991); D. Allasia et al., Phys. Lett. **249B**, 366 (1990).
- [48] K. Gottfried, Phys. Rev. Lett. **18**, 1174 (1967).
- [49] S. Kumano, SAGA-HE-97-97, Feb. 1997.
- [50] M. Glück, E. Reya and A. Vogt, Z. Phys C **67**, 433 (1995).
- [51] H.L. Lai et al., Phys. Rev. D **51**, 4763 (1995).
- [52] F.A. Berends, R. Kleiss and S. Jadach, Nucl. Phys. **B202**, 63 (1982), and references therein.
- [53] F. Abe et al., Phys. Rev. Lett. **67**, 1502 (1991); N.A. Graf, FERMILAB-Conf-96/454-E, Jan. 1997.

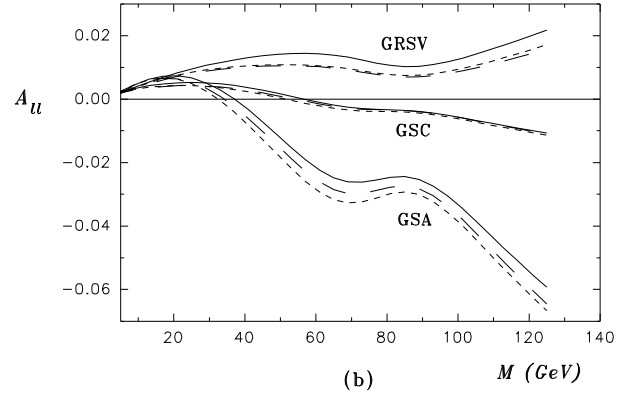
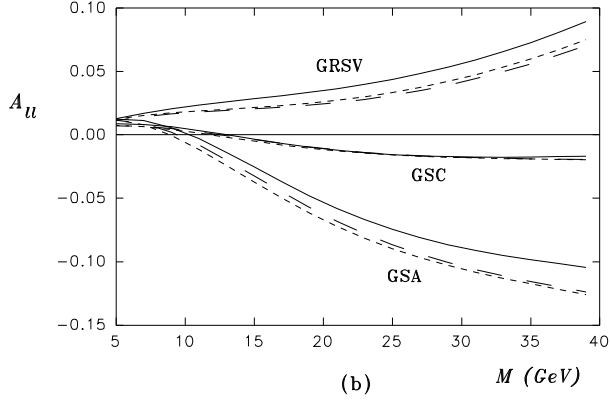
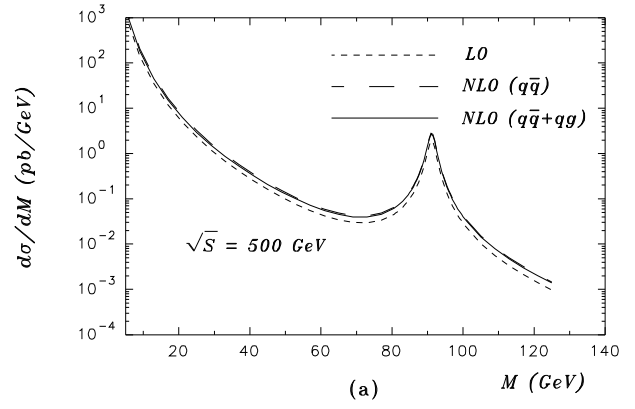
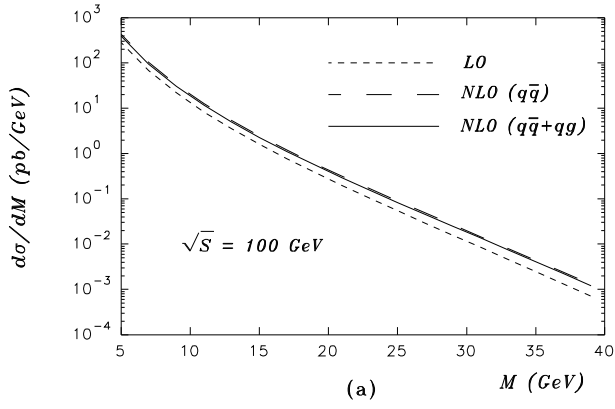


FIG. 1. (a) The cross section, $d\sigma/dM$, versus M , for l^+l^- production in pp collisions at $\sqrt{S} = 100$ GeV; (b) corresponding double-spin asymmetry, $A_{\ell\ell}$, for various sets of polarized parton distributions. Details given in text.

FIG. 3. (a) The cross section, $d\sigma/dM$, versus M , for l^+l^- production in pp collisions at $\sqrt{S} = 500$ GeV; (b) corresponding double-spin asymmetry, $A_{\ell\ell}$, for various sets of polarized parton distributions. Lines as in Fig. 1.

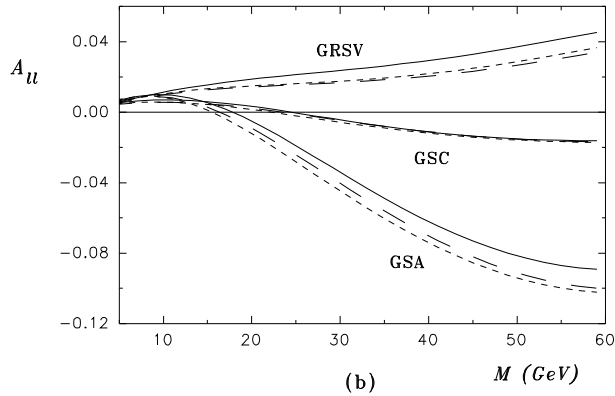
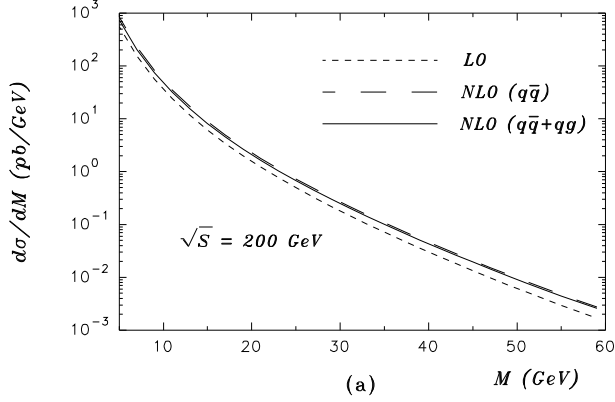


FIG. 2. As Fig. 1, except at $\sqrt{S} = 200$ GeV.

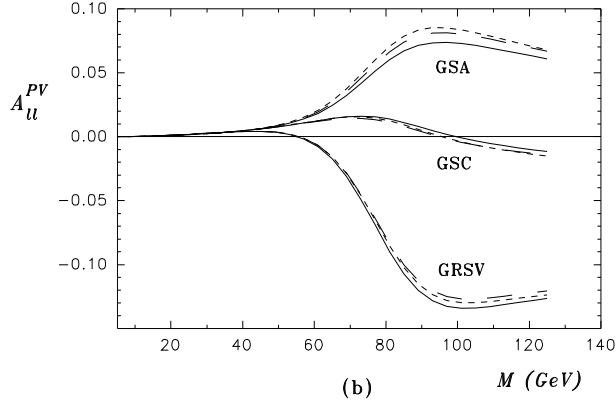
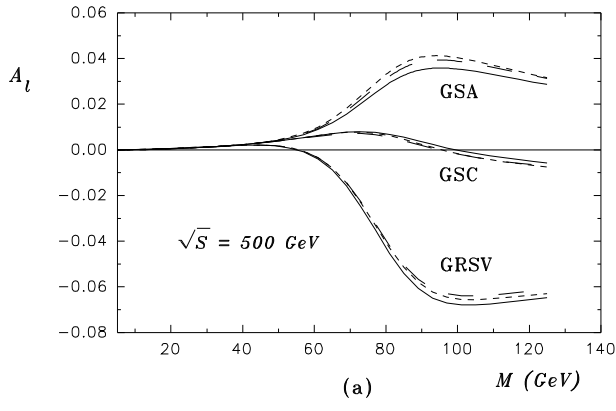


FIG. 4. (a) The single-spin asymmetry, A_l , versus M , for l^+l^- production in pp collisions at $\sqrt{S} = 500$ GeV; (b) corresponding two-spin parity violating asymmetry, A_{ll}^{PV} . Lines as in Fig. 1.

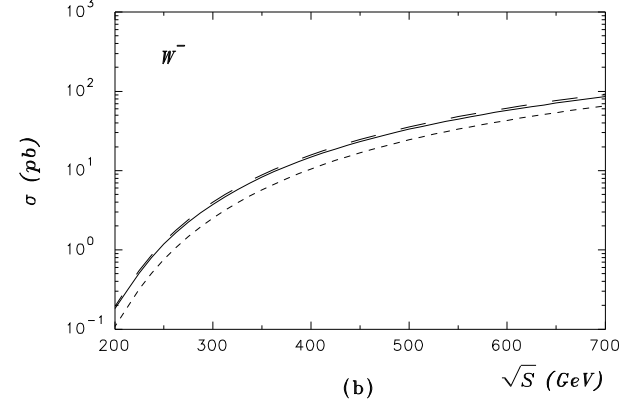
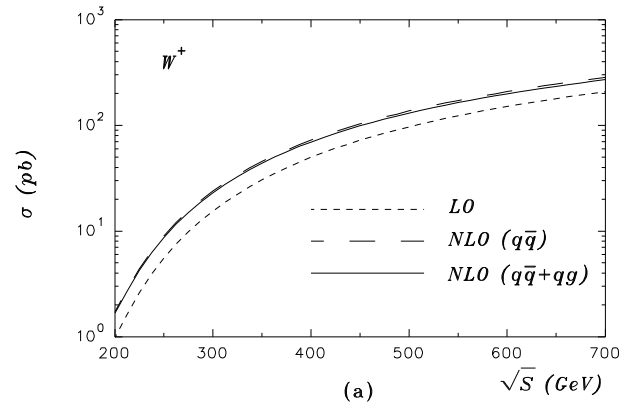


FIG. 5. (a) The total cross section for $W^+(\rightarrow l^+\nu_l)$ production, versus \sqrt{S} , in pp collisions; (b) corresponding cross section for $W^-(\rightarrow l^-\bar{\nu}_l)$ production. Lines as in Fig. 1.

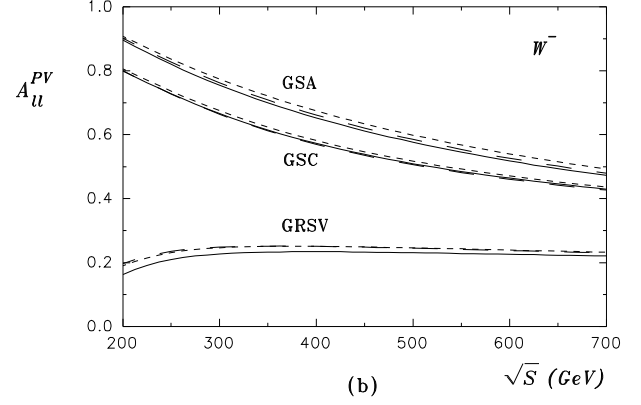
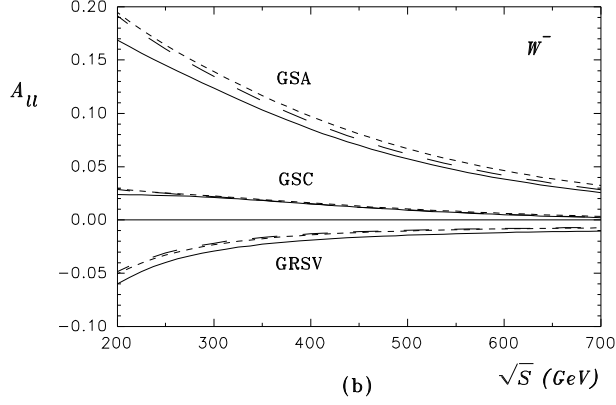
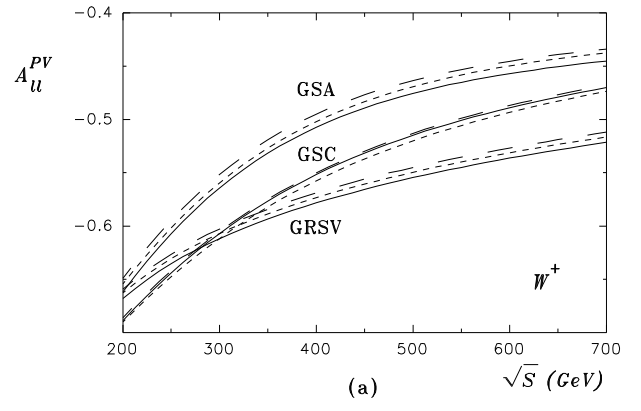
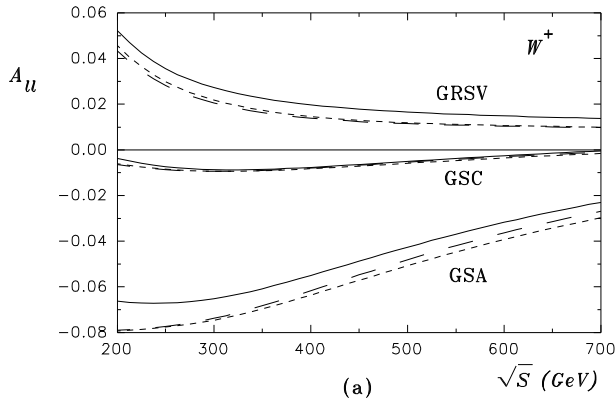


FIG. 6. (a) The double-spin asymmetry, A_u , for $W^+(\rightarrow l^+\nu_l)$ production in pp collisions, versus \sqrt{S} ; (b) corresponding asymmetry for $W^-(\rightarrow l^-\bar{\nu}_l)$ production. Lines as in Fig. 1.

FIG. 8. As Fig. 6, except here the two-spin parity violating asymmetry, A_u^{PV} , is plotted.

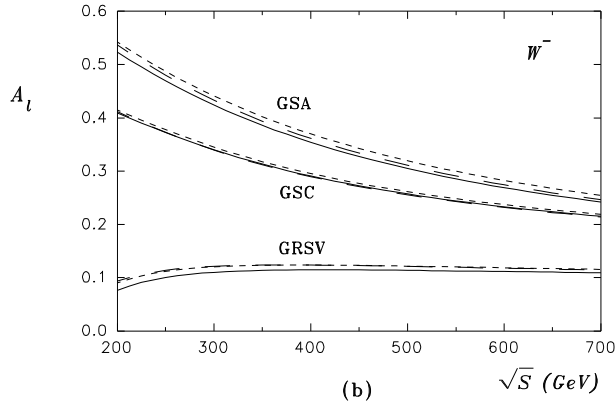
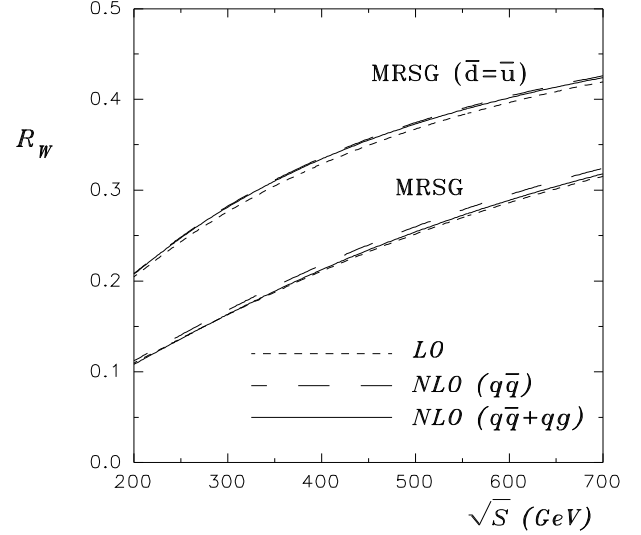
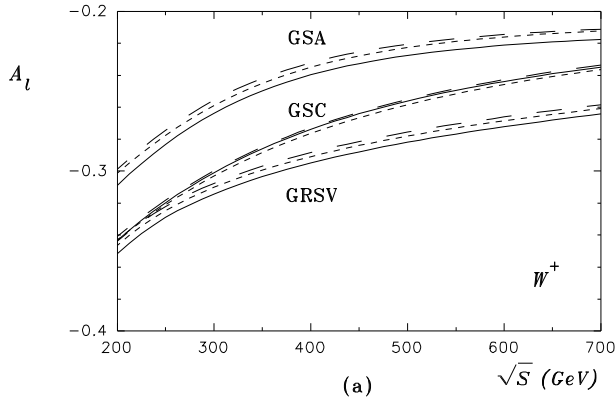


FIG. 9. The ratio of the $W^-(\rightarrow l^-\bar{\nu}_l)$ to $W^+(\rightarrow l^+\nu_l)$ cross sections, R_W , versus \sqrt{S} , in pp collisions. Predictions are made using both the MRSG set and the MRSG set with the \bar{d} distribution set equal to the \bar{u} distribution. Lines as in Fig. 1.

FIG. 7. As Fig. 6, except here the single-spin asymmetry, A_l , is plotted.

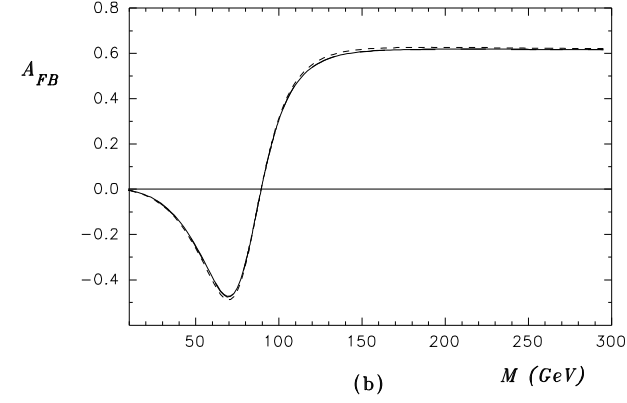
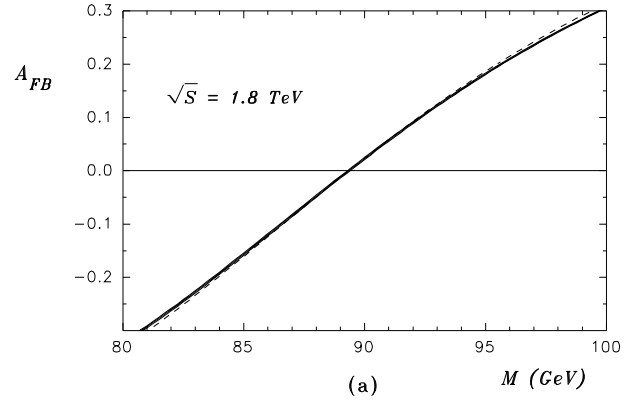
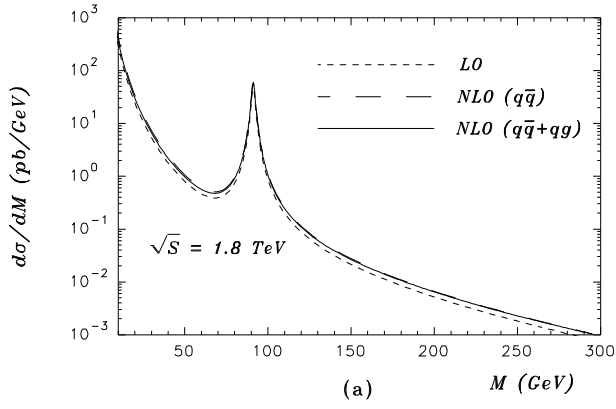


FIG. 10. (a) The cross section, $d\sigma/dM$, versus M , for l^+l^- production in $p\bar{p}$ collisions at $\sqrt{S} = 1.8$ TeV; (b) corresponding forward-backward lepton asymmetry, A_{FB} , obtained using $\sin^2 \theta_W = .2315$. Lines as in Fig. 1.

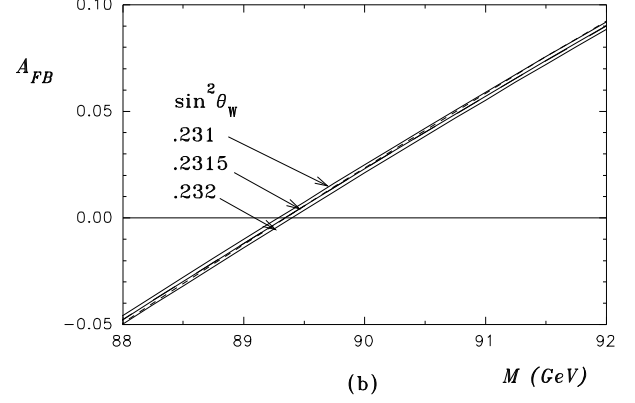


FIG. 12. (a) The A_{FB} of Fig. 10(b), but in the mass region, $80 \leq M \leq 100$ GeV. The effect of varying $\sin^2 \theta_W$ by $\pm .0005$, on A_{FB}^{NLO} , is shown. (b) Same as (a), but in the mass region, $88 \leq M \leq 92$ GeV.

TABLE I. The $\Delta_k T_{ij}$ which define the various factorization schemes of interest; here $k = u, l$.

	$\overline{\text{MS}}$	$\overline{\text{MS}}_\varepsilon$	$\overline{\text{MS}}_{HC}$	$\overline{\text{MS}}_p$
$\Delta_k T_{qq}$	0	$\Delta_k P_{qq}^\varepsilon$	$\Delta_l P_{qq}^\varepsilon - \Delta_u P_{qq}^\varepsilon$	$\Delta_l P_{qq}^\varepsilon - \Delta_u P_{qq}^\varepsilon$
$\Delta_k T_{qg}$	0	$\Delta_k P_{qg}^\varepsilon$	0	$\Delta_l P_{qg}^\varepsilon$
$\Delta_k T_{gq}$	0	$\Delta_k P_{gq}^\varepsilon$	0	$\Delta_l P_{gq}^\varepsilon$
$\Delta_k T_{gg}$	0	$\Delta_k P_{gg}^\varepsilon$	0	$\Delta_l P_{gg}^{\varepsilon, <}$

FIG. 11. The ratio, A_{FB}^{NLO}/A_{FB}^{LO} , using the $A_{FB}^{(N)LO}$ of Fig. 10(b).